Int. J. Solids Structures Vol. 25, No. 7, pp. 803–833, 1989
Printed in Great Britain.

0020-7683/89 $3.00 + .00

ON ENERGY-BASED COUPLED ELASTOPLASTIC DAMAGE THEORIES: CONSTITUTIVE MODELING AND COMPUTATIONAL ASPECTS

J. W. JU
Department of Civil Engineering and Operations Research, Princeton University, Princeton, NJ 08544, U.S.A.

(*Received* 16 *July* 1988; *in revised form* 6 *December* 1988)

Abstract—Novel energy-based coupled elastoplastic damage theories are presented in this paper. The proposed formulation employs irreversible thermodynamics and internal state variable theory for ductile and brittle materials. At variance with Lemaitre's work on damage-elastoplasticity, the present formulation renders rational thermodynamic potential and damage energy release rate. In contrast to previous work by Simo and Ju (featuring an additive split of the stress tensor), current formulation assumes an additive split of the strain tensor. It is shown that the "strain split" damage-elastoplasticity formulation leads to more robust tangent moduli than the "stress split" formulation. The plastic flow rule and hardening law are characterized in terms of the effective quantities; *viz.* the *effective stress space plasticity*. This mechanism is both physically well-motivated and computationally efficient. Further, a fourth-order anisotropic damage mechanism is proposed for brittle materials. Rational mechanisms are also presented to account for the microcrack opening and closing operations as well as the strain-rate dependency of microcrack growth.

Efficient computational algorithms for proposed elastoplastic damage models are subsequently explored by making use of the "operator splitting" methodology. In particular, new three-step operator split algorithms are presented. Application is made to a class of inviscid and rate-dependent cap-damage models for concrete and mortar. Experimental validations are also given to illustrate the applicability of the proposed damage models.

1. INTRODUCTION

The inelastic behavior of the mechanical constitutive responses of engineering materials is in general related to the irreversible thermodynamic processes involving energy dissipation and stiffness variation due to physical changes in the microstructure. Some commonly employed inelastic theories include, for instance, viscoelasticity, plasticity and damage mechanics. In the past two decades, in particular, the damage mechanics approach has emerged as a viable framework for the description of distributed material damage including material stiffness degradation, microcrack initiation, growth and coalescence, as well as damage-induced anisotropy, etc. Damage mechanics has been applied to model creep damage (Hult, 1974; Kachanov, 1958, 1981, 1984; Krajcinovic, 1983a; Leckie and Hayhurst, 1974; Lemaitre, 1984; Murakami, 1981; Rabotnov, 1963), fatigue damage (Chaboche, 1974; Lemaitre, 1971, 1984; Marigo, 1985), creep fatigue interaction (Lemaitre, 1984; Lemaitre and Chaboche, 1974; Lemaitre and Plumtree, 1979), elasticity coupled with damage (Cordebois and Sidoroff, 1979; Ju *et al.*, 1989; Kachanov, 1980, 1987a,b; Krajcinovic and Fonseka, 1981; Ortiz, 1985; Wu, 1985), and ductile plastic damage (Cordebois and Sidoroff, 1982; Dragon, 1985; Dragon and Chihab, 1985; Lemaitre and Dufailly, 1977; Lemaitre, 1984, 1985, 1986; Simo and Ju, 1987a,b,c). In addition, damage mechanics has been introduced to describe the inelastic behavior of brittle materials such as concrete and rock (Francois, 1984; Ilankamban and Krajcinovic, 1987; Kachanov, 1982; Krajcinovic, 1983b; Krajcinovic and Fonseka, 1981; Loland, 1980; Lorrain and Loland, 1983; Mazars, 1982, 1986; Mazars and Lemaitre, 1984; Resende and Martin, 1984; Simo and Ju, 1987a, b).

Recently, micromechanical damage theories are proposed in the literature to model non-interacting microcrack growth in an originally isotropic linear elastic brittle solid; see, e.g. Wu (1985), Krajcinovic and Fanella (1986), Sumarac and Krajcinovic (1987) (which extends the work of Horii and Nemat-Nasser (1983) to a process model). In the case of nonlinear elastoplasticity coupled with many distributed interacting microcracks, nevertheless, such micromechanical derivation of microcrack kinetic laws presents tremendous

difficulties and challenges, and is an objective for future research. Further, as was remarked by Krajcinovic (1985), a purely micromechanical theory may never replace a properly formulated phenomenological theory as a design tool.

Continuum damage mechanics is based on the thermodynamics of irreversible processes, the internal state variable theory and relevant physical considerations (e.g. the assumption of distributed microcracks, homogenization concept, the definition of micromechanical damage variable, kinetic law of damage growth, nonlocal damage characterization and plasticity-damage coupling mechanism, etc.). A scalar damage variable is suitable for characterizing (homogenized) isotropic damage processes. Nevertheless, a tensor-valued damage variable (fourth order) is necessary in order to account for anisotropic damage effects.

Many researchers in damage mechanics focused on the linear "elastic-damage" mechanics for brittle materials; i.e. linear elastic solids with distributed microcracks. For nonlinearly elastic solids and elastoplastic solids, nonetheless, their methods are not applicable in general. By contrast, some elastoplastic damage theories have been proposed (e.g. Lemaitre, 1984, 1985, 1986; Dragon, 1985; Simo and Ju, 1987a, b, c). However, it appears that the thermodynamic free energy function and the "damage energy release rate" proposed by Lemaitre (1985) may not be physically appropriate. In fact, the theory advocated by Lemaitre implies that the thermodynamic force conjugate to elastoplastic microcrack evolution is simply the elastic strain energy, i.e. plastic strains do not contribute to the microcrack growth process. On the other hand, the theory proposed by Dragon (1985) does not offer thermodynamic damage energy criteria, nor provide tangent moduli or numerical simulations or experimental validations. Hence, coupled elastoplastic damage mechanics warrants further study.

It is important to clarify the term "damage" employed in the current literature. As was pointed out by Krajcinovic, there are at least three different levels of scale of "damage" in material mechanical responses: (a) atomic voids and crystal lattice defects, which require the use of non-continuum mechanics models at the atomic scale; (b) microcracks and microvoids, which require micromechanical damage models (to model microstructural changes and individual microcracks growth) or phenomenological continuum damage models (to model distributed microcracks); and (c) macrocracks, which warrant fracture mechanics models to model the growth of discrete macrocracks.

In this paper, novel energy-based (isotropic or anisotropic) coupled elastoplastic damage theories are presented to characterize distributed microcracks (not ductile microvoids) in brittle damage modes [including "Cleavage 1", "Cleavage 2" and "Cleavage 3" in the sense of Ashby (1979)]. An outline of the paper is as follows. In Section 2, the definitions of "damage variable" are reviewed; the homogenization concept and alternative nonlocal damage definition are discussed; and the basic hypotheses of damage mechanics developed are summarized. In Section 3 energy-based isotropic elastoplastic damage theories are given, which are capable of accommodating nonlinear elastic response and general plastic response. The proposed theories can predict degradation in both elastic and plastic material properties (such as elastic moduli and plastic flow stresses). At variance with Lemaitre's formulation, a new free energy function and proper "damage energy release rate" are constructed.

In contrast to previous work by Simo and Ju (1987a, b, c) (which features an additive split of the stress tensor), this paper assumes an additive split of the strain tensor into the "elastic damage" and "plastic-damage" parts from the outset. It is shown that the current "strain split" damage-plasticity formulation is physically more appealing (analogous to the J-integral in nonlinear fracture mechanics) and results in more robust tangent moduli than the "stress split" formulation. In addition, the plastic flow rule and hardening law are characterized in terms of the effective stress quantities; namely, the *effective stress space plasticity*. A rate-dependent damage mechanism is subsequently developed to account for the microcrack retardation effects at higher strain rates. Rational mechanism is also proposed to simulate the "mode I" microcrack opening and closing operations.

The framework constructed in Section 3 is further extended in Section 4 to develop simple energy-based fourth-order anisotropic damage models for brittle materials.

Recognizing the important role played by constitutive algorithms in constitutive theories and modeling, computational aspects of the proposed elastoplastic damage models are systematically explored in Section 5. In particular, new three-step operator split algorithms are developed within the present framework. Application is made to a class of inviscid and rate-dependent cap-damage models for concrete and mortar in Section 6. Experimental validations are also given to illustrate the applicability of proposed damage models and algorithms.

2. A FRAMEWORK FOR DAMAGE MECHANICS

Physically, degradation of material properties is related to the initiation, growth and coalescence of microcracks or microvoids. Some basic concepts pertaining to damage mechanics are reviewed in this section.

2.1. *Damage variable and homogenization*

"Damage" can be defined as a collection of permanent microstructural changes concerning material thermomechanical properties (e.g. stiffness, strength, anisotropy, etc.) brought about in a material by a set of irreversible physical microcracking processes resulting from the application of thermomechanical loadings (Talreja, 1985). The selection of a "damage" variable should be based on proper micromechanical considerations. For several types of material microstructure, microcracks develop in characteristic patterns and the microstructure can be assumed to be statistically homogeneous. These patterned damages are observed in fibrous composite laminates, concrete and ceramics (Weitsman, 1987). Several definitions of damage are possible for consideration. For example,

(i) Define the second-order damage tensor $\mathbf{D}$ as a spatial average:

$$\mathbf{D} \equiv \frac{1}{2V} \sum_k \int_{S^{(k)}} (\mathbf{b} \otimes \mathbf{n} + \mathbf{n} \otimes \mathbf{b})^{(k)} \, dS^{(k)} \tag{1}$$

in which $\mathbf{b}$ and $\mathbf{n}$ denote the displacement discontinuity vector ($\mathbf{b} \equiv [\mathbf{u}]$) and the unit normal vector across the kth microcrack surface $S^{(k)}$, respectively (Vakulenko and Kachanov, 1971; Dragon, 1985). The representative volume V is a proper statistical and micromechanical measure for observing or computing an overall constitutive law. The minimum prescription for the representative unit cell is that the magnitude of local wave-like fluctuations about the expected (mean) values of phase variables should not depend on the size of the unit cell so that the system is macroscopically homogeneous (Hill, 1967, 1972). At the macroscopic level, V plays the role of an infinitesimal material neighborhood with uniform state variables. At the microscale, however, V plays the role of a "micro-continuum" with nonuniform spatial variables (Eringen, 1968; Ortiz, 1987a). However, as pointed out by Krajcinovic (1985), the definition (1) is thermodynamically incorrect because it leads to energy dissipation during unloading. Equation (1) is, nevertheless, a good index for "added flexibility" (damage-induced inelastic strain) due to open microcracks.

(ii) Define the damage variable $d_{\mathbf{n}}$ (in the normal direction $\mathbf{n}$) as

$$d_{\mathbf{n}} \equiv \frac{A_d}{A_T} \tag{2}$$

where A_d is the damaged surface area (taking into account the microcrack area, the microstress concentration and the interaction between microcracks) and A_T is the total cross-sectional area of a surface of a unit cell along a normal direction $\mathbf{n}$ (see, e.g. Lemaitre, 1984, 1985). The definition of a damage variable can also be anisotropic to signify different oriented geometry and micro-defects in material bonding; e.g. three changing principal normal directions of a three-dimensional oriented microcrack.

(iii) Define the damage measure d as (assuming only one single microcrack)

$$d \equiv \frac{a^3}{V}. \tag{3}$$

where a is the radius of an assumed single spherical microcrack and V is the volume of a representative unit cell in the mesostructure (see, e.g. Budiansky and O'Connell, 1976; Wu, 1985; Krajcinovic, 1987). This definition is related to the microcrack porosity (concentration ratio) within the unit cell. It is emphasized that eqn (3) can lead to a fourth-order damage tensor representation.

The homogenization procedure can be applied not only to damage variables but also to stresses and strains. For instance, one may write

$$\hat{\boldsymbol{\sigma}} \equiv \frac{1}{V}\int_V \boldsymbol{\sigma}\, dv; \quad \hat{\boldsymbol{\varepsilon}} \equiv \frac{1}{V}\int_V \boldsymbol{\varepsilon}\, dv. \tag{4}$$

2.2. *Alternative nonlocal damage characterization*

As was noted earlier, the state variables display non-uniform spatial fluctuations at the microscale. Therefore, nonlocal continuum theory may be considered for damage mechanics (see, e.g. Bazant *et al.*, 1987; Eringen, 1983, 1987; Eringen and Edelen, 1972; Pijaudier-Cabot and Bazant, 1987; Xia *et al.*, 1987). The essence of nonlocal theory includes the characteristic length (l) and the "attenuation" (weighting) function ($\omega(\mathbf{x})$). It is noted that nonlocal spatial averaging is fundamentally different from the homogenization concept, although nonlocal theory might provide a unified foundation for the homogenization concept. ω contains a crucial material parameter — the characteristic length which is generally influenced by the spacing, size and shape of inclusions (or aggregates, fibers). In the event of inhomogeneous anisotropic materials, one could replace the homogeneous isotropic attenuation function $\omega(\mathbf{x})$ by a fourth-order attenuation tensor $\omega_{ijkl}(\mathbf{x})$.

2.3. *Effective stress concept and hypothesis of strain equivalence*

Let us denote by $\mathbf{M}$ a fourth-order tensor which characterizes the state of damage and transforms the homogenized stress tensor $\boldsymbol{\sigma}$ into the effective stress tensor $\tilde{\boldsymbol{\sigma}}$; *viz.*

$$\tilde{\boldsymbol{\sigma}} \equiv \mathbf{M}^{-1} : \boldsymbol{\sigma}. \tag{5}$$

For isotropic damage case, the mechanical behavior of microcracks is independent of their orientation and depends only on a scalar variable d. Accordingly, $\mathbf{M}$ simply reduces to $(1-d)\mathbf{I}$, where $\mathbf{I}$ is the rank four identity tensor, and (5) collapses to

$$\tilde{\boldsymbol{\sigma}} \equiv \frac{\boldsymbol{\sigma}}{1-d}. \tag{6}$$

The coefficient $(1-d)$ dividing the stress tensor in (6) is a reduction factor associated with the amount of damage in the material first introduced by Kachanov (1958). The value $d = 0$ corresponds to the undamaged state, $d = d_c$ defines the complete local rupture ($d_c \in [0, 1]$), and $d \in (0, d_c)$ corresponds to a partially damaged state. Local stresses are redistributed to the undamaged material micro-bonds and therefore the effective stresses are higher than the nominal stresses. In addition, Lemaitre introduced the following hypothesis of strain equivalence: "The strain associated with a damaged state under the applied stress is equivalent to the strain associated with its undamaged state under the effective stress." See Fig. 1 for a schematic explanation.

Remark 2.3.1. *Added flexibility*. Due to the existence of microcracks, the flexibility of a material increases. To see this, consider for simplicity the elastic-damage case (see Fig.

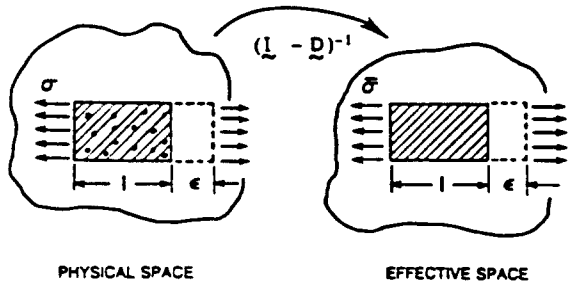

Fig. 1. Hypothesis of strain equivalence.

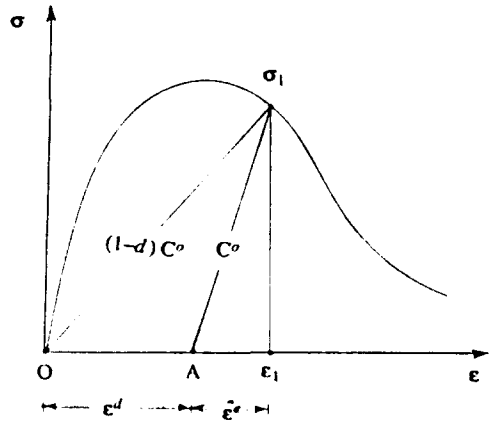

Fig. 2. Illustration of added flexibility. $\tilde{\varepsilon}^e$ and ε^d denote the truly elastic strain and added deformation due to microcracks, respectively.

2). Let us denote by $\mathbf{C}^o$ the undamaged stiffness and $(1-d)\mathbf{C}^o$ the damaged unloading stiffness (as will be derived in eqn (21)). It is assumed that all microcracks close upon unloading and therefore no permanent deformation exists upon complete unloading. Accordingly, the truly reversible (elastic) strain is obtained by following the unloading slope $\mathbf{C}^o$ and is designated as $\tilde{\boldsymbol{\varepsilon}}^e$. It is observed from Fig. 2 that the gap between point O and point A is actually the inelastic strain $\boldsymbol{\varepsilon}^d$ due to microcrack opening during the loading process. See also Ortiz (1985). □

3. ENERGY-BASED ISOTROPIC ELASTOPLASTIC DAMAGE MODELS

The underlying concept of the energy-based elastoplastic damage models presented in this section is that damage in a material is linked to the history of both elastic and plastic state variables. The framework constructed in this section will be extremely useful in the development of anisotropic damage models proposed in Section 4.

The fundamental problem of the ductile plastic damage formulation advocated by Lemaitre (1984, 1985, 1986) is the non-optimal choice of the locally averaged free energy potential. In particular, damage is associated only with the elastic strains and the damage energy release rate is shown to be the elastic strain energy in Lemaitre (1985). This treatment amounts to uncoupled plasticity and damage processes, thus in a sense contradicting experimental evidence that plastic variables also contribute to the initiation and growth of microcracks. By contrast, a new free energy function and damage energy release rate are proposed in this section. The damage energy release rate (energy barrier) controls the microcrack propagation and arrest. The damage loading/unloading conditions are completely characterized by this energy barrier which is related to the local debonding energy required to initiate or propagate microcracks. The notion of effective stress and the hypothesis of strain equivalence are also utilized.

3.1. *Thermodynamic basis. Strain split*

The split of the total strain tensor into the "elastic-damage" and "plastic-damage" parts is assumed at the outset; i.e.

$$\boldsymbol{\varepsilon} = \boldsymbol{\varepsilon}^e + \boldsymbol{\varepsilon}^p. \tag{7}$$

It is emphasized that the "added flexibility" due to the existence of microcracks is already embedded in $\boldsymbol{\varepsilon}^e$ and $\boldsymbol{\varepsilon}^p$ implicitly (see Remark 2.3.1). That is, $\boldsymbol{\varepsilon}^e$ ($\boldsymbol{\varepsilon}^p$) includes not only the truly elastic (plastic) strain but also the added deformation due to active microcracks. Upon complete unloading, however, we assume that all microcracks are closed and no residual strain is induced by micro-defects. To introduce both damage and plasticity mechanisms, let us consider the following locally averaged (homogenized) free energy function:

$$\Psi(\boldsymbol{\varepsilon}^e, \mathbf{q}, d) \equiv (1-d)\Psi^o(\boldsymbol{\varepsilon}^e, \mathbf{q}) \tag{8}$$

where $\mathbf{q}$ denotes a suitable set of plastic variables and $\Psi^o(\boldsymbol{\varepsilon}^e, \mathbf{q})$ signifies the total potential energy function of an undamaged (virgin) material. One often assumes (although unnecessary) that the elastic and plastic potential energy functions are uncoupled; i.e. $\Psi^o(\boldsymbol{\varepsilon}^e, \mathbf{q}) \equiv \Psi^o_e(\boldsymbol{\varepsilon}^e) + \Psi^o_p(\mathbf{q})$.

Confining our attention to the purely mechanical theory, the Clausius–Duhem inequality takes the form

$$-\dot{\Psi} + \boldsymbol{\sigma} : \dot{\boldsymbol{\varepsilon}} \geqslant 0 \tag{9}$$

for any admissible process. Taking time derivative of eqn (8), substituting into (9), and making use of standard arguments (Coleman and Gurtin, 1967) along with the additional assumption that damage and plastic unloading are elastic processes, we obtain

$$\boldsymbol{\sigma} = \frac{\partial \Psi}{\partial \boldsymbol{\varepsilon}^e} = (1-d)\frac{\partial \Psi^o}{\partial \boldsymbol{\varepsilon}^e} \tag{10}$$

and the dissipative inequalities

$$\Psi^o(\boldsymbol{\varepsilon}^e, \mathbf{q})\dot{d} \geqslant 0 \quad \text{and} \quad \frac{\partial \Psi^o}{\partial \boldsymbol{\varepsilon}^e} : \dot{\boldsymbol{\varepsilon}}^p - \frac{\partial \Psi^o}{\partial \mathbf{q}} \cdot \dot{\mathbf{q}} \geqslant 0. \tag{11}$$

It is clear from eqns (10) and (11) that the present framework is capable of accommodating nonlinear elastic response and general plastic response. Moreover, it is noted that the effective stress is given by the expression

$$\tilde{\boldsymbol{\sigma}} = \frac{\boldsymbol{\sigma}}{1-d} = \frac{\partial \Psi^o(\boldsymbol{\varepsilon}^e, \mathbf{q})}{\partial \boldsymbol{\varepsilon}^e}. \tag{12}$$

Remark 3.1.1. From eqn (8) it follows that

$$-Y \equiv -\frac{\partial \Psi(\boldsymbol{\varepsilon}^e, \mathbf{q}, d)}{\partial d} = \Psi^o(\boldsymbol{\varepsilon}^e, \mathbf{q}). \tag{13}$$

Therefore, we conclude that the undamaged energy function $\Psi^o(\boldsymbol{\varepsilon}^e, \mathbf{q})$ is the thermodynamic force (damage energy release rate) conjugate to the damage variable d. This is at variance with Cordebois and Sidoroff (1982) and Lemaitre (1984, 1985, 1986), who considered only the elastic part of the damage energy, $\Psi^o_e(\boldsymbol{\varepsilon}^e)$. It is noted that by considering the elastic damage energy only is physically incorrect since plastic dissipation is not properly accounted for. See also Chow and Wang (1987a) for more anomalies of elastic damage energy release rate. □

Remark 3.1.2. A different formulation based on an additive split of the stress tensor was previously proposed by Simo and Ju (1987a, b). In their work, the thermodynamic damage energy release rate was shown to be $\Psi^0(\boldsymbol{\varepsilon})$; i.e. the total undamaged stored energy function with the total strain tensor $\boldsymbol{\varepsilon}$ as its argument. By contrast, the damage energy release rate in the present formulation is $\Psi^0(\boldsymbol{\varepsilon}^e, \mathbf{q})$ which is smaller than $\Psi^0(\boldsymbol{\varepsilon})$. It is interesting to notice that $\Psi^0(\boldsymbol{\varepsilon}^e, \mathbf{q})$ is actually the local counterpart of the global J-integral fracture energy in nonlinear elastoplastic fracture mechanics. This is not the case of the alternative quantity $\Psi^0(\boldsymbol{\varepsilon})$ proposed by Simo and Ju (1987a, b). □

3.2. *Characterization of damage*

A simple isotropic elastoplastic damage mechanism is characterized in this section to describe the progressive degradation of mechanical properties of materials. Motivated by Remark 3.1.1, we propose to employ the (locally averaged) undamaged energy function Ψ^0 (the damage energy release rate) to characterize the damage loading/unloading conditions. For convenience, we define the notation ξ as

$$\xi \equiv \Psi^0(\boldsymbol{\varepsilon}^e, \mathbf{q}). \tag{14}$$

The state of damage in the material is then characterized by means of a damage criterion $g(\xi_t, r_t) \leqslant 0$ with the following functional form:

$$g(\xi_t, r_t) \equiv \xi_t - r_t \leqslant 0, \quad t \in \mathbb{R}_+. \tag{15}$$

Here, the subscript t refers to the value at current time $t \in \mathbb{R}_+$, and r_t signifies damage threshold (energy barrier) at current time t (i.e. the radius of the damage surface). If r_0 denotes the initial damage threshold before any loading is applied, a property characteristic of the material, we must have $r_t \geqslant r_0$. Condition (15) then states that damage in the material is initiated when the damage energy release rate (ξ_t) exceeds the initial damage threshold r_0. The above energy-based damage criterion is fundamentally linked to the history of both elastic and plastic variables. A large body of current literatures, however, adopts certain stress-based damage criteria; see, e.g. Chow and Wang (1987a, b) (which tried to remedy Cordebois and Sidoroff, 1982). It is noted that a stress-based damage criterion in the presence of significant plastic flows is inherently inadequate for predicting realistic plastic damage growth. To substantiate this statement, let us consider for simplicity the perfect plasticity coupled with damage. The effective stresses are constant and the homogenized stresses are decreasing; consequently, a stress-based criterion will not predict significant damage accumulation even under large plastic deformations.

To describe the growth of microcracks and the expansion of damage surfaces, it is necessary to specify the equations of evolution for d and r. As was mentioned earlier, micromechanical derivation of microcrack kinetic growth laws is currently achievable only in the case of originally homogeneous, linear isotropic elastic solids without microcrack interaction. In the case of general nonlinear elastoplasticity coupled with interacting microcracks, such micromechanical derivation is not available yet. Hence, in this section, a phenomenological description of the kinetics of microcrack growth is attempted. For the isotropic damage case, we define the evolution equations as

$$\begin{aligned} \dot{d}_t &= \dot{\mu} H(\xi_t, d_t, s, a, c, \rho) \\ \dot{r}_t &= \dot{\mu} \end{aligned} \tag{16}$$

where s is the spacing of inclusions (fibers or aggregates), a the grain size, c the microcrack size, and ρ the porosity (e.g. water/cement ratio in concrete). In addition, $\dot{\mu} \geqslant 0$ is a damage consistency parameter which defines damage loading/unloading conditions according to the Kuhn–Tucker relations:

$$\dot{\mu} \geqslant 0, \quad g(\xi_t, r_t) \leqslant 0, \quad \dot{\mu} g(\xi_t, r_t) = 0. \tag{17a-c}$$

Conditions (17) are standard for problems involving unilateral constraint. If $g(\xi_t, r_t) < 0$, the damage criterion is not satisfied and by condition (17c) we have $\dot{\mu} = 0$; hence, the damage rule (16) implies that $\dot{d} = 0$ and no further damage takes place. If, on the other hand $\dot{\mu} > 0$, that is further damage is taking place, condition (17c) now implies that $g(\xi_t, r_t) = 0$. In this event the value of $\dot{\mu}$ is determined by the "damage consistency condition"; i.e.

$$g(\xi_t, r_t) = \dot{g}(\xi_t, r_t) = 0 \Rightarrow \dot{\mu} = \dot{\xi}_t. \tag{18}$$

So that r_t is given by the expression

$$r_t = \max\left\{r_0, \max_{\tau \in (-\infty, t]} \xi_\tau\right\}. \tag{19}$$

3.2.1. *Elastic-damage tangent moduli.* For isotropic ductile damage, the above characterization of damage results in symmetric elastic-damage tangent moduli. In the absence of further plastic flow, $\dot{\boldsymbol{\varepsilon}}^p \equiv \dot{\mathbf{q}} \equiv \mathbf{0}$. Time differentiation of (10) along with the damage rule (16) and the damage consistency condition (18) then yield

$$\dot{\boldsymbol{\sigma}} = (1-d)\frac{\partial^2 \Psi^e(\boldsymbol{\varepsilon}^e, \mathbf{q})}{\partial \boldsymbol{\varepsilon}^{e2}} : \dot{\boldsymbol{\varepsilon}} - H\dot{\xi}\bar{\boldsymbol{\sigma}} \tag{20}$$

where $\bar{\boldsymbol{\sigma}} \equiv \partial \Psi^e / \partial \boldsymbol{\varepsilon}^e$ (the effective stress) and, for notational simplicity, the subscript t has been dropped. By taking the time derivative of eqn (14), we obtain $\dot{\xi} = \bar{\boldsymbol{\sigma}} : \dot{\boldsymbol{\varepsilon}}$. Substitution into (20) then yields $\dot{\boldsymbol{\sigma}} = \mathbf{C}(\boldsymbol{\varepsilon}^e, \mathbf{q}, d) : \dot{\boldsymbol{\varepsilon}}$, where $\mathbf{C}(\boldsymbol{\varepsilon}^e, \mathbf{q}, d)$ is the elastic-damage tangent modulus given by

$$\mathbf{C}(\boldsymbol{\varepsilon}^e, \mathbf{q}, d) \equiv \left[(1-d)\frac{\partial^2 \Psi^e(\boldsymbol{\varepsilon}^e, \mathbf{q})}{\partial \boldsymbol{\varepsilon}^{e2}} - H\bar{\boldsymbol{\sigma}} \otimes \bar{\boldsymbol{\sigma}}\right]. \tag{21}$$

Note that $\mathbf{C}(\boldsymbol{\varepsilon}^e, \mathbf{q}, d)$ is a symmetric rank four tensor. It is often assumed that the undamaged tangent modulus $\mathbf{C}^e \equiv \partial^2 \Psi^e / \partial \boldsymbol{\varepsilon}^{e2}$ is constant.

3.3. *Coupled elastoplastic damage response*

Once microcracks occur, local stresses are redistributed to undamaged material micro-bonds over the effective area. Thus, true stresses of undamaged material points are higher than nominal stresses. Accordingly, it appears reasonable to state that the plastic flows occur only in the undamaged material micro-bonds by means of effective quantities. In fact, this is simply the underlying notion of the effective stress concept. Therefore, the characterization of the plastic response should be formulated in the effective stress space in terms of effective quantities $\bar{\boldsymbol{\sigma}}$ and $\mathbf{q}$. The homogenized stress tensor $\boldsymbol{\sigma}$ is replaced by the effective stress tensor $\bar{\boldsymbol{\sigma}}$ in the stress space yield criterion; i.e. the "elastic-damage" domain is defined by $f(\bar{\boldsymbol{\sigma}}, \mathbf{q}) \leqslant 0$. It is recognized that due to the existence of microcracks the plastic flow stresses and plastic material properties degrade. Use of effective quantities in the yield condition essentially has the net effect of lowering the plastic strength and flow stresses of materials. By assuming an associative flow rule, the rate-independent damaged plastic response is characterized as follows:

$$\dot{\boldsymbol{\varepsilon}}^p = \dot{\lambda}\frac{\partial f}{\partial \bar{\boldsymbol{\sigma}}}(\bar{\boldsymbol{\sigma}}, \mathbf{q}) \quad (\textit{flow rule}) \tag{22a}$$

$$\dot{\mathbf{q}} = \dot{\lambda}\mathbf{h}(\bar{\boldsymbol{\sigma}}, \mathbf{q}) \quad (\textit{plastic hardening law}) \tag{22b}$$

$$f(\bar{\boldsymbol{\sigma}}, \mathbf{q}) \leqslant 0 \quad (\textit{yield condition}) \tag{22c}$$

where $\dot{\lambda}$ denotes the plastic consistency parameter and $\mathbf{h}$ signifies the vectorial hardening function. It is interesting to notice that in spite of the normality rule assumption (22a) in

the effective stress space $\bar{\boldsymbol{\sigma}}$, the flow rule direction *departs* from normality in the homogenized stress space $\boldsymbol{\sigma}$ in the case of anisotropic damage. Hence, the damage-perturbed yield criterion and damage-induced non-associative flow rule (despite the associative flow rule in terms of $\bar{\boldsymbol{\sigma}}$) are accounted for in eqns (22). Further, the loading/unloading conditions can be expressed in a compact form by requiring that

$$f(\bar{\boldsymbol{\sigma}}, \mathbf{q}) \leqslant 0, \quad \dot{\lambda} \geqslant 0, \quad \dot{\lambda} f(\bar{\boldsymbol{\sigma}}, \mathbf{q}) = 0. \tag{23}$$

$\dot{\lambda}$ is determined by requiring that $\dot{f} = 0$, the so-called plastic consistency condition. Hence, during plastic loading one has

$$\frac{\partial f}{\partial \bar{\boldsymbol{\sigma}}} : \dot{\bar{\boldsymbol{\sigma}}} + \frac{\partial f}{\partial \mathbf{q}} \cdot \dot{\mathbf{q}} = 0. \tag{24}$$

For simplicity, we shall assume uncoupled elastic and plastic potential energy functions; namely, $\Psi^o(\boldsymbol{\varepsilon}^e, \mathbf{q}) \equiv \Psi^o_e(\boldsymbol{\varepsilon}^e) + \Psi^o_p(\mathbf{q})$. Therefore, from eqn (10) we obtain

$$\dot{\bar{\boldsymbol{\sigma}}} = \frac{\partial^2 \Psi^o}{\partial \boldsymbol{\varepsilon}^{e2}} : \dot{\boldsymbol{\varepsilon}}^e = \frac{\partial^2 \Psi^o}{\partial \boldsymbol{\varepsilon}^{e2}} : \left(\dot{\boldsymbol{\varepsilon}} - \dot{\lambda} \frac{\partial f}{\partial \bar{\boldsymbol{\sigma}}} \right) \tag{25}$$

where use has been made of the flow rule (22a). Thus, $\dot{\lambda}$ is determined as

$$\dot{\lambda} = \frac{\dfrac{\partial f}{\partial \bar{\boldsymbol{\sigma}}} : \dfrac{\partial^2 \Psi^o}{\partial \boldsymbol{\varepsilon}^{e2}} : \dot{\boldsymbol{\varepsilon}}}{\dfrac{\partial f}{\partial \bar{\boldsymbol{\sigma}}} : \dfrac{\partial^2 \Psi^o}{\partial \boldsymbol{\varepsilon}^{e2}} : \dfrac{\partial f}{\partial \bar{\boldsymbol{\sigma}}} - \dfrac{\partial f}{\partial \mathbf{q}} \cdot \mathbf{h}}. \tag{26}$$

Substitution of (26) into (25) then yields $\dot{\bar{\boldsymbol{\sigma}}} = \bar{\mathbf{C}}^{ep} : \dot{\boldsymbol{\varepsilon}}$, where $\bar{\mathbf{C}}^{ep}$ is the effective elastoplastic tangent modulus (a symmetric fourth-order tensor) given by

$$\bar{\mathbf{C}}^{ep} \equiv \frac{\partial^2 \Psi^o}{\partial \boldsymbol{\varepsilon}^{e2}} - \frac{\left[\dfrac{\partial^2 \Psi^o}{\partial \boldsymbol{\varepsilon}^{e2}} : \dfrac{\partial f}{\partial \bar{\boldsymbol{\sigma}}} \right] \otimes \left[\dfrac{\partial^2 \Psi^o}{\partial \boldsymbol{\varepsilon}^{e2}} : \dfrac{\partial f}{\partial \bar{\boldsymbol{\sigma}}} \right]}{\dfrac{\partial f}{\partial \bar{\boldsymbol{\sigma}}} : \dfrac{\partial^2 \Psi^o}{\partial \boldsymbol{\varepsilon}^{e2}} : \dfrac{\partial f}{\partial \bar{\boldsymbol{\sigma}}} - \dfrac{\partial f}{\partial \mathbf{q}} \cdot \mathbf{h}}. \tag{27}$$

To derive the elastoplastic-damage tangent moduli, we recall that $\boldsymbol{\sigma} = (1-d)\bar{\boldsymbol{\sigma}}$. Time differentiation then leads to

$$\dot{\boldsymbol{\sigma}} = (1-d)\dot{\bar{\boldsymbol{\sigma}}} - \dot{d}\bar{\boldsymbol{\sigma}} = (1-d)\bar{\mathbf{C}}^{ep} : \dot{\boldsymbol{\varepsilon}} - \dot{\xi} H \bar{\boldsymbol{\sigma}} \tag{28}$$

where use has been made of eqns (16) and (18). In addition, the time derivative of eqn (14) along with eqns (22) yields

$$\dot{\xi} = \bar{\boldsymbol{\sigma}} : (\dot{\boldsymbol{\varepsilon}} - \dot{\boldsymbol{\varepsilon}}^p) + \frac{\partial \Psi^o}{\partial \mathbf{q}} \cdot \dot{\mathbf{q}} = \bar{\boldsymbol{\sigma}} : \dot{\boldsymbol{\varepsilon}} - \dot{\lambda} \left[\bar{\boldsymbol{\sigma}} : \frac{\partial f}{\partial \bar{\boldsymbol{\sigma}}} - \frac{\partial \Psi^o}{\partial \mathbf{q}} \cdot \mathbf{h} \right]. \tag{29}$$

Substitution of eqns (26) and (29) into (28) then renders $\dot{\boldsymbol{\sigma}} = \mathbf{C}^{ep} : \dot{\boldsymbol{\varepsilon}}$. Here $\mathbf{C}^{ep}$ is the elastoplastic-damage tangent modulus given by

$$\mathbf{C}^{ep} = (1-d)\bar{\mathbf{C}}^{ep} - H[\bar{\boldsymbol{\sigma}} \otimes \bar{\boldsymbol{\sigma}}] + \frac{H\left(\bar{\boldsymbol{\sigma}} : \dfrac{\partial f}{\partial \bar{\boldsymbol{\sigma}}} - \dfrac{\partial \Psi^o}{\partial \mathbf{q}} \cdot \mathbf{h} \right)}{\dfrac{\partial f}{\partial \bar{\boldsymbol{\sigma}}} : \dfrac{\partial^2 \Psi^o}{\partial \boldsymbol{\varepsilon}^{e2}} : \dfrac{\partial f}{\partial \bar{\boldsymbol{\sigma}}} - \dfrac{\partial f}{\partial \mathbf{q}} \cdot \mathbf{h}} \left[\bar{\boldsymbol{\sigma}} \otimes \left(\frac{\partial^2 \Psi^o}{\partial \boldsymbol{\varepsilon}^{e2}} : \frac{\partial f}{\partial \bar{\boldsymbol{\sigma}}} \right) \right]. \tag{30}$$

It is observed from eqn (30) that $\mathbf{C}^{ep}$ is in general a non-symmetric rank four tensor. Nevertheless, in the particular event in which we have constant (linear) $\mathbf{C}^0 \equiv \partial^2\Psi^e/\partial\boldsymbol{\varepsilon}^{e2}$ and von Mises J_2-plasticity, $\mathbf{C}^{ep}$ in eqn (30) is symmetric. The above coupled elastoplastic-damage formulation can be readily extended to accommodate non-associative flow rules (in the effective stress space $\bar{\boldsymbol{\sigma}}$) by simply replacing f in eqn (22a) by a suitable plastic potential $Q(\bar{\boldsymbol{\sigma}}, \mathbf{q})$.

Remark 3.3.1. A damage-perturbed yield criterion and damage-induced non-associative flow rule in the homogenized stress space $\boldsymbol{\sigma}$ was proposed by Dragon (1985). It is noted, however, that two different yield functions are used in Dragon (1985) to define the "genuine" yield potential and another damage-perturbed pseudo-potential, respectively. The tangent moduli are always non-symmetric. Moreover, the corresponding elastoplastic-damage return mapping algorithms are rather cumbersome due to two simultaneous consistency conditions. □

Remark 3.3.2. For the derivation of $\dot{\lambda}$ in eqn (26) we have assumed that $\Psi^e(\boldsymbol{\varepsilon}^e, \mathbf{q}) \equiv \Psi_e^e(\boldsymbol{\varepsilon}^e) + \Psi_p^e(\mathbf{q})$. If this is not the case, the denominator in eqns (26) and (27) should be replaced by the following expression:

$$\left[\frac{\partial f}{\partial \bar{\boldsymbol{\sigma}}} : \frac{\partial^2\Psi^e}{\partial \boldsymbol{\varepsilon}^{e2}} : \frac{\partial f}{\partial \bar{\boldsymbol{\sigma}}} - \frac{\partial f}{\partial \bar{\boldsymbol{\sigma}}} : \frac{\partial^2\Psi^e}{\partial \boldsymbol{\varepsilon}^e \partial \mathbf{q}} \cdot \mathbf{h} - \frac{\partial f}{\partial \mathbf{q}} \cdot \mathbf{h}\right]. \quad \square \tag{31}$$

Remark 3.3.3. In the previous work by Simo and Ju (1987a, b), the formulation hinges on an additive split of the stress tensor. As a result, their elastoplastic-damage tangent moduli $\mathbf{C}^{ep}$ are always non-symmetric even with $\mathbf{C}^e$ constant. In addition, in the case of nonlinear elasticity (either physically or geometrically) coupled with damage-plasticity, the elastic and elastoplastic-damage tangent moduli ($\partial^2\Psi^e(\boldsymbol{\varepsilon})/\partial\boldsymbol{\varepsilon}^2$ and $\mathbf{C}^{ep}$) are too "soft" due to the fact that the argument of differentiation is the total strain tensor $\boldsymbol{\varepsilon}$ (see eqn (24) in Simo and Ju, 1987a; see also Simo and Ju, 1987c for the finite deformation case). These "soft" tangent moduli could lead to numerical difficulties when large strains are encountered. By contrast, the present formulation employs more robust (stiffer) elastic tangent moduli $\partial^2\Psi^e(\boldsymbol{\varepsilon}^e, \mathbf{q})/\partial\boldsymbol{\varepsilon}^{e2}$ and elastoplastic-damage tangent moduli $\mathbf{C}^{ep}$, with the elastic strain tensor $\boldsymbol{\varepsilon}^e$ as the argument of differentiation. This advantage together with our J-integral-like damage energy release rate ($\Psi^e(\boldsymbol{\varepsilon}^e, \mathbf{q})$) make the present formulation computationally and physically more attractive. □

Remark 3.3.4. *Selection of* $\Psi^e(\boldsymbol{\varepsilon}^e, \mathbf{q})$. The specific forms of the undamaged free energy function Ψ^e depend on the mechanical behavior and thermodynamic process of materials. From eqn (11), it is observed that the thermodynamic forces conjugate to $\dot{\boldsymbol{\varepsilon}}^p$ and $\dot{\mathbf{q}}$ are $\partial\Psi^e/\partial\boldsymbol{\varepsilon}^e$ (or simply $\bar{\boldsymbol{\sigma}}$) and $-(\partial\Psi^e/\partial\mathbf{q})$, respectively. In fact, in eqn (22a), the partial derivative is taken with respect to $\bar{\boldsymbol{\sigma}}$. Therefore, it appears rational to postulate that

$$\dot{\mathbf{q}} \equiv \dot{\lambda} \frac{\partial f}{\partial\left(-\dfrac{\partial\Psi^e}{\partial\mathbf{q}}\right)}. \tag{32}$$

By comparing eqn (32) with (22b), we obtain the relation

$$\mathbf{h}(\bar{\boldsymbol{\sigma}}, \mathbf{q}) = -\frac{\partial f}{\partial\left(\dfrac{\partial\Psi^e}{\partial\mathbf{q}}\right)}. \tag{33}$$

For demonstration purpose, let us assume that $\Psi^e(\boldsymbol{\varepsilon}^e, \mathbf{q}) = \Psi_e^e(\boldsymbol{\varepsilon}^e) + \Psi_p^e(\mathbf{q})$ and consider the von Mises plasticity with linear isotropic hardening. Thus, we have $\mathrm{d}\Psi_p^e/\mathrm{d}\bar{\varepsilon}^p = R(\bar{\varepsilon}^p)$, with

$\bar{\varepsilon}^p$ and $R(\bar{\varepsilon}^p)$ signifying the equivalent plastic strain and yield radius, respectively. Hence, we arrive at $\Psi_p^o = \int_0^{\bar{\varepsilon}^p} R(\bar{\varepsilon}^p)\,\mathrm{d}\bar{\varepsilon}^p$. For linear hardening, $R(\bar{\varepsilon}^p) = R_o + \theta\bar{\varepsilon}^p$, with R_o and θ denoting the initial yield radius and slope, respectively. Accordingly, $\Psi_p^o(\bar{\varepsilon}^p) = R_o\bar{\varepsilon}^p + \frac{1}{2}\theta\bar{\varepsilon}^{p2}$. For other plasticity models, one could assume that $\Psi^o = \int_0^{\varepsilon} \bar{\boldsymbol{\sigma}} : \mathrm{d}\boldsymbol{\varepsilon}$ and compute Ψ^o incrementally. On the other hand, the form of Ψ_e^o hinges on the particular hyperelasticity model employed; e.g. for linear elasticity case, one has $\Psi_e^o(\boldsymbol{\varepsilon}^e) = \frac{1}{2}\boldsymbol{\varepsilon}^e : \mathbf{C}^o : \boldsymbol{\varepsilon}^e$. □

3.4. *Rate-dependent damage mechanism*

Some experimental results (on rocks and concrete) show that the amount of microcracking at a particular strain level exhibits rate sensitivity to the applied rate of loading in a dynamic environment. Further, strain-softening and loss of strong ellipticity phenomena associated with damage mechanisms impose numerical difficulties in finite element computations. To account for rate dependency and to regularize the localization problems, a viscous damage mechanism is presented in this section. It is noted that the structure of this regularization is analogous to the viscoplastic regularization of the Perzyna type (Perzyna, 1966). In particular, rate equations governing visco-damage behavior are obtained from their rate-independent counterpart, eqn (16), by replacing the damage consistency parameter $\dot{\mu}$ by $\mu\bar{\phi}(g)$. Here μ is the damage viscosity coefficient, $\bar{\phi}(g)$ denotes the viscous damage flow function and g is defined in eqn (15). With this at hand, we write

$$\begin{aligned} \dot{d}_i &= \mu\langle\bar{\phi}(g)\rangle H(\xi_i, d_i, s, a, c, \rho) \\ \dot{r}_i &= \mu\langle\bar{\phi}(g)\rangle \end{aligned} \tag{34}$$

where $\langle\cdot\rangle$ denotes the McAuley bracket. In the event of linear viscous damage mechanism (i.e. $\bar{\phi}(g) \equiv g$), eqn (34) then takes the form

$$\begin{aligned} \dot{d}_i &= \mu\langle g\rangle H(\xi_i, d_i, s, a, c, \rho) \\ \dot{r}_i &= \mu\langle g\rangle \equiv \mu\langle\xi_i - r_i\rangle. \end{aligned} \tag{35}$$

The above viscous mechanism is capable of predicting retardation in microcrack growth at higher strain rates. In addition, the inviscid damage characterization can be recovered by letting μ go to infinity. On the other hand, as μ approaches zero we obtain the instantaneous elastic response (in the absence of plastic flow).

3.5. *Microcrack opening and closing*

Although the damage models presented in Sections 3.3 and 3.4 are isotropic, they can be easily extended to account for the "mode I" microcrack opening and closing effects. Let us start by considering the spectral decomposition of the strain tensor (see also Ortiz, 1985)

$$\boldsymbol{\varepsilon} = \sum_{i=1}^{3} \varepsilon_i \mathbf{p}_i \otimes \mathbf{p}_i, \quad |\mathbf{p}_i| = 1 \tag{36}$$

where ε_i is the ith principal strain and $\mathbf{p}_i$ the ith corresponding unit principal direction. Let $\mathbf{Q}$ and $\mathbf{Q}^+$, separately, be the regular and positive (tensile) spectral projection tensors defined as

$$\mathbf{Q} \equiv \sum_{i=1}^{3} \mathbf{p}_i \otimes \mathbf{p}_i; \quad \mathbf{Q}^+ \equiv \sum_{i=1}^{3} \hat{H}(\varepsilon_i)\mathbf{p}_i \otimes \mathbf{p}_i \tag{37}$$

where $\hat{H}(\cdot)$ is the Heaviside ramp function. We now introduce the fourth-order positive projection tensor $\mathbb{P}^+$ with components

$$\mathbb{P}^+_{ijkl} = Q^+_{ia} Q^+_{jb} Q_{ka} Q_{lb} \tag{38}$$

so that $\boldsymbol{\varepsilon}^+$ can be expressed as (see also Ortiz, 1985)

$$\boldsymbol{\varepsilon}^+ = \mathbb{P}^+ : \boldsymbol{\varepsilon}, \quad \text{i.e.} \quad \varepsilon_{ij}^+ = P_{ijkl}^+ \varepsilon_{kl}. \tag{39}$$

It is observed that $\mathbb{P}^+$ depends on the total strain $\boldsymbol{\varepsilon}$.

With these notations at hand, eqn (10) is then rephrased to take into account the active (open) microcracks under tensile extensions. Specifically, we write

$$\boldsymbol{\sigma} = (\mathbf{I} - \mathbf{D}^{\text{act}}) : \frac{\partial \Psi^e}{\partial \boldsymbol{\varepsilon}^e} \tag{40}$$

where $\mathbf{D}^{\text{act}} \equiv d\mathbb{P}^+\mathbb{P}^+ = d\mathbb{P}^+\mathbb{P}^+$ is the fourth-order active anisotropic damage tensor. If all three principal strains ε_i are tensile, then we have $\mathbb{P}^+ = \mathbf{I}$ and $\mathbf{D}^{\text{act}} = d\mathbf{I}$; i.e. the local microcrack is open (active) in all three principal directions and we recover isotropic damage under current state. If all ε_i are compressive, then $\mathbb{P}^+ = \mathbf{0}$ and $\mathbf{D}^{\text{act}} = \mathbf{0}$; i.e. the local microcrack is entirely closed (passive) under current state. Clearly, other combinations of tensile and compressive states will give rise to various microcrack opening and closing situations.

The damage energy release rate $\xi \equiv \Psi^e$ in eqn (14) can also be modified as follows to accommodate ductile and brittle (tensile) material damage.

$$\xi \equiv \begin{cases} \Psi^e(\boldsymbol{\varepsilon}^e, \mathbf{q}) & (\textit{ductile}) \\ \Psi^e(\boldsymbol{\varepsilon}^{e+}, \mathbf{q}) & (\textit{brittle}) \end{cases} \tag{41}$$

where $\boldsymbol{\varepsilon}^{e+} \equiv \mathbb{P}^+ : \boldsymbol{\varepsilon}^e$.

Remark 3.5.1. The above discussion on microcrack closure, eqns (36)–(40), is quite similar to the proposal of Ortiz (1985). However, there are some subtle differences between the two formulations. First, the explicit form of the positive orthogonal projection tensor $\mathbb{P}^+$ in eqn (38) is more precise than that given in Ortiz (1985) (see eqn (3.60) therein). Second, the present discussion employs the description of stiffness degradation through the active damage tensor $\mathbf{D}^{\text{act}}$ while Ortiz (1985) used the "added compliance" characterization $\mathbf{C}^e$ (see eqns (3.11)–(3.14) in Ortiz, 1985). Third, $\mathbb{P}^+$ in eqn (38) is a nonlinear, non-constant operator associated with the current total strain tensor $\boldsymbol{\varepsilon}$. In Ortiz (1985), by contrast, there are really two distinct orthogonal projections involved (see eqns (3.9) and (3.60) therein). Specifically, the first one is $\mathbb{P}_\varepsilon^+$ associated with the current strain tensor $\boldsymbol{\varepsilon}$; i.e. $\boldsymbol{\varepsilon}^+ \equiv \mathbb{P}_\varepsilon^+ : \boldsymbol{\varepsilon}$. The other one is $\mathbb{P}_\sigma^+$ associated with the current stress tensor $\boldsymbol{\sigma}$; i.e. $\boldsymbol{\sigma}^+ \equiv \mathbb{P}_\sigma^+ : \boldsymbol{\sigma}$ (see also eqn (3.18) in Ortiz, 1987b). In general, $\mathbb{P}_\varepsilon^+$ is *not* equal to $\mathbb{P}_\sigma^+$. It appears that this distinction was not made clear in Ortiz (1985). In addition, in a strain-driven algorithm, $\boldsymbol{\sigma}$ is yet unknown before local constitutive iteration. Hence, use of $\mathbb{P}_\sigma^+$ introduces more computational efforts. Fourth, due to the existence of two distinct orthogonal projections in Ortiz (1985), eqns (3.11)–(3.14) therein seem unclear. In particular, eqn (3.13) in Ortiz (1985) could be interpreted as

$$\mathbf{C}^e = \mathbb{P}_\varepsilon^+ : \bar{\mathbf{C}}^e : \mathbb{P}_\sigma^+. \tag{42}$$

Accordingly, the active "added compliance" $\mathbf{C}^e$ becomes a non-symmetric tensor and eqn (3.14) in Ortiz (1985) might be questionable because $\boldsymbol{\sigma}^+$ is not equal to $\mathbb{P}_\varepsilon^+ : \boldsymbol{\sigma}$. In the present proposal, on the other hand, only one orthogonal projection $\mathbb{P}^+$ (see eqn (38)) is needed and no confusion ever arises. □

4. ENERGY-BASED ANISOTROPIC ELASTOPLASTIC DAMAGE MODELS

The energy-based damage models developed in Section 3 are extended in this section to account for anisotropic brittle microcracking effects. In view of the significance of tensile extensions in brittle damage processes, proper damage characterization via tensile spectral decomposition is employed.

To illustrate the physical motivation of the proposed energy-based anisotropic brittle damage model, consider the idealized situation of a cylinder subject to unconfined increasing uniaxial compression. The objective is to simulate the "splitting mode". By properly including the tensile radial and hoop strains contribution to damage and screening out the compressive axial strain contribution, the proposed mechanism would predict progressive microcracking parallel to the axis of loading (normal to the plane of tensile lateral strains) and ultimate failure of the specimen. This is a typical failure mode in many rock-like materials such as concrete. Note that a damage model based on tensile stresses could not possibly predict such a failure mode.

4.1. *Thermodynamic basis*

The proposed damage characterization is based on the concept of effective stress and features a simple and effective construction of the fourth-order transformation tensor $\mathbf{M}$ in eqn (5). In fact, one could define $\mathbf{M} \equiv \mathbf{I} - \mathbf{D}$ (see also Cordebois and Sidoroff, 1982). The damaged secant (unloading) stiffness tensor then takes the form $\mathbf{C} = (\mathbf{I} - \mathbf{D})\mathbf{C}^0$, where $\mathbf{C}^0$ is the undamaged linear elasticity tensor. It is observed that the damaged stiffness $\mathbf{C}$ possesses a one-to-one correspondence with the fourth-order damage tensor $\mathbf{D}$. Hence, one could equivalently define $\mathbf{C}$ as the anisotropic damage variable. In addition, it is realized that $\mathbf{M} \equiv \mathbf{C}\mathbf{C}^{0\,-1}$.

As a point of departure, we postulate the following locally averaged free energy:

$$\Psi(\boldsymbol{\varepsilon}^e, \mathbf{q}, \mathbf{C}) \equiv \Psi_{ed}(\boldsymbol{\varepsilon}^e, \mathbf{C}) + \Psi_{pd}(\mathbf{q}, \mathbf{C}) = \tfrac{1}{2}\boldsymbol{\varepsilon}^e : \mathbf{C} : \boldsymbol{\varepsilon}^e + \Psi_{pd}(\mathbf{q}, \mathbf{C}). \tag{43}$$

The Clausius–Duhem inequality then leads to

$$\dot{\boldsymbol{\varepsilon}} : [\boldsymbol{\sigma} - \mathbf{C} : \boldsymbol{\varepsilon}^e] - \left[\tfrac{1}{2}\boldsymbol{\varepsilon}^e : \dot{\mathbf{C}} : \boldsymbol{\varepsilon}^e + \frac{\partial \Psi_{pd}}{\partial \mathbf{C}} : \dot{\mathbf{C}}\right] + \left[\boldsymbol{\varepsilon}^e : \mathbf{C} : \dot{\boldsymbol{\varepsilon}}^p - \frac{\partial \Psi_{pd}}{\partial \mathbf{q}} \cdot \dot{\mathbf{q}}\right] \geqslant 0. \tag{44}$$

Therefore, we obtain the following stress–strain relation

$$\boldsymbol{\sigma} = \frac{\partial \Psi}{\partial \boldsymbol{\varepsilon}} = \mathbf{C} : \boldsymbol{\varepsilon}^e \tag{45}$$

along with the following damage and plastic dissipation inequalities

$$\mathbb{D}^d \equiv -\tfrac{1}{2}\boldsymbol{\varepsilon}^e : \dot{\mathbf{C}} : \boldsymbol{\varepsilon}^e - \frac{\partial \Psi_{pd}}{\partial \mathbf{C}} : \dot{\mathbf{C}} \geqslant 0 \tag{46}$$

$$\mathbb{D}^p \equiv \boldsymbol{\sigma} : \dot{\boldsymbol{\varepsilon}}^p - \frac{\partial \Psi_{pd}}{\partial \mathbf{q}} \cdot \dot{\mathbf{q}} \geqslant 0. \tag{47}$$

In addition, from eqn (46) and the fact that

$$-\mathbf{Y} \equiv \frac{\partial \Psi}{\partial \mathbf{C}} = \tfrac{1}{2}\boldsymbol{\varepsilon}^e \otimes \boldsymbol{\varepsilon}^e + \frac{\partial \Psi_{pd}}{\partial \mathbf{C}} \tag{48}$$

we conclude that $[\frac{1}{2}\boldsymbol{\varepsilon}^e \otimes \boldsymbol{\varepsilon}^e + (\partial \Psi_{pd}/\partial \mathbf{C})]$ is the thermodynamic force conjugate to the damaged secant (unloading) stiffness $\mathbf{C}$. This thermodynamic force physically defines the "anisotropic damage energy release rate" and will be used to characterize damage evolution.

In particular, we shall assume that Ψ_{pd} is linear in $\mathbf{D}$ (or $\mathbf{C}$); e.g.

$$\Psi_{pd}(\mathbf{q}, \mathbf{C}) \equiv [(\mathbf{I} - \mathbf{D}) : \mathbf{I}]\tilde{\Psi}_p^0(\mathbf{q}) \tag{49}$$

where $\tilde{\Psi}_p^0(\mathbf{q}) \equiv \frac{1}{6}\Psi_p^0(\mathbf{q})$, the undamaged plastic free energy potential. Accordingly, we have

$\partial \Psi_{pd}/\partial \mathbf{C} = \tilde{\Psi}_p''(\mathbf{q})\mathbf{C}''^{-1}$. Equation (48) can then be rephrased as

$$-\mathbf{Y} \equiv \frac{\partial \Psi}{\partial \mathbf{C}} = \tfrac{1}{2}\boldsymbol{\varepsilon}^e \otimes \boldsymbol{\varepsilon}^e + \tilde{\Psi}_p''(\mathbf{q})\mathbf{C}''^{-1}. \tag{50}$$

4.2. *Characterization of brittle damage*

To account for the nature of irreversibility during microcracking processes, a damage criterion in terms of the anisotropic damage debonding-energy release rate $(-\mathbf{Y})$ is proposed as follows

$$g \equiv \hat{G}(-\mathbf{Y}, s, a, c, \rho) - r_t \leqslant 0 \tag{51}$$

where $\hat{G}$ is a function of the arguments. The damage process is then characterized in terms of the following irreversible, dissipative equations of evolution

$$\dot{\mathbf{C}} = -\dot{\mu}\frac{\partial g}{\partial(-\mathbf{Y})}$$

$$\dot{\mu} \geqslant 0, \quad g \leqslant 0, \quad \dot{\mu} g \equiv 0. \tag{52}$$

Equation (52) can be regarded as the Kuhn–Tucker conditions of the following "principle of maximum damage energy dissipation": "For a given local strain history, the actual damaged modulus $\mathbf{C}$ is the modulus that renders *maximum* damage energy dissipation". This principle is analogous to the principle of maximum plastic dissipation.

To properly include the anisotropic damage energy release rate $-\mathbf{Y}$ in the damage criterion (51) and the damage evolution equations (52), it is essential to define the characteristic damage measure ξ such that

$$\frac{\partial \xi}{\partial(-\mathbf{Y})} \equiv \mathbb{P}^+ \mathbf{C}''' \mathbb{P}^+ \tag{53}$$

where $\mathbb{P}^+$ is defined in eqn (38). For an isotropic linear elasticity tensor $\mathbf{C}''$, this warrants the following definition of ξ

$$\xi \equiv \tfrac{1}{2}\boldsymbol{\varepsilon}^{e+} : \mathbf{C}'' : \boldsymbol{\varepsilon}^{e+} + \tilde{\Psi}_p'' \left\{ \frac{(\frac{1}{3}G - K)}{6KG}\, \mathbf{I} : [\mathbb{P}^+ \mathbf{C}'' \mathbb{P}^+] : \mathbf{I} + \frac{1}{2G} \sum_{i=1}^{9} \mathbf{e}_i : [\mathbb{P}^+ \mathbf{C}'' \mathbb{P}^+] : \mathbf{e}_i \right\} \tag{54}$$

in which $\mathbf{e}_i$ is the ith unit base tensor of the identity tensor $\mathbf{I}$, and K and G are the bulk and shear moduli, respectively. With this notation at hand, eqn (51) is recast as follows.

$$g \equiv \tilde{G}(\xi, s, a, c, \rho) - r_t \leqslant 0. \tag{55}$$

In addition, we define $H \equiv \partial \tilde{G}/\partial \xi$ and $\dot{r}_t \equiv \dot{\mu} H$. From eqn (55), it is observed that $\dot{r}_t \equiv \dot{\xi} H$ in the event of damage loading. Hence, we obtain $\dot{\mu} = \dot{\xi}$. The anisotropic damage (microcrack) evolution equation (52) then becomes

$$\dot{\mathbf{C}} = -\dot{\xi} H \mathbb{P}^+ \mathbf{C}'' \mathbb{P}^+. \tag{56}$$

It is emphasized that only tensile extensions in the principal directions contribute to microcrack growth according to eqn (56). Physically, this treatment corresponds to anisotropic (oriented) brittle microcrack propagation. Clearly, the crucial quantities are ξ and $\mathbb{P}^+$. Note that $(\mathrm{d}/\mathrm{d}t)(\mathbb{P}^+ : \boldsymbol{\varepsilon}) \neq \mathbb{P}^+ : \dot{\boldsymbol{\varepsilon}}$ owing to the nonlinear nature of $\mathbb{P}^+$.

Remark 4.2.1. The anisotropic damage evolution rule (52) can be viewed as an extension of an earlier proposal in Ortiz (1985) (for mortar). There exist, nevertheless, several sig-

nificant differences between the two formulations, which are as follows. (i) Ortiz (1985) assumed that the rate of irreversible (plastic) deformation is coaxial with the total rate of inelastic deformation (consisting of contributions of increasing damage and increasing permanent deformations). This assumption is not utilized in the present formulation. (ii) Ortiz's (1985) formulation focused on the rate of "added compliance" tensor while the present proposal focuses on the rate of "damaged secant (unloading) stiffness" tensor. It is emphasized that the two procedures are not equivalent. (iii) The "perfectly brittle" and "plastic microcracking" damage models in Ortiz (1985) are really stress-based. That is, the damage criterion and damage flow rule are based on the current stress tensor ($\boldsymbol{\sigma}$ or $\boldsymbol{\sigma}^+$); see eqns (3.30), (3.34), (3.41), (3.47) in Ortiz (1985). In particular, plastic (permanent) strains do not contribute to the damage criterion $\Phi(\boldsymbol{\sigma}, \mu)$ in Ortiz's models. As previously discussed in Section 3.2, stress-based damage criterion is inherently inadequate for coupled damage-elastoplasticity when plastic deformation is significant. □

Remark 4.2.2. Within the present context, plastic response can be characterized independently from the damage evolution in terms of effective stress quantities exactly as in Section 3.3. □

Remark 4.2.3. A rate-dependent anisotropic damage mechanism can be constructed analogous to the formulation proposed in Section 3.4. In essence, we have the following evolution equations (see eqn (34)):

$$\dot{\mathbf{C}} = -\mu\langle\bar{\phi}(g)\rangle H \mathbb{P}^+ \mathbf{C}^e \mathbb{P}^+ \tag{57}$$

$$\dot{r}_t = \mu\langle\bar{\phi}(g)\rangle H. \qquad \square \tag{58}$$

Remark 4.2.4. The "mode I" microcrack opening and closing mechanisms can be easily accommodated within the proposed anisotropic damage framework. First, we define the "total stiffness loss tensor" as

$$\mathbf{C}^d \equiv \int_0^t (-\dot{\mathbf{C}})\, dt. \tag{59}$$

Then we define the "active stiffness loss tensor" $\mathbf{C}^d_{act}$ (due to open microcracks) and the "active damaged secant stiffness tensor" $\mathbf{C}^{act}$ as follows:

$$\mathbf{C}^d_{act} \equiv \mathbb{P}^+ \mathbf{C}^d \mathbb{P}^+ \tag{60}$$

$$\mathbf{C}^{act} \equiv \mathbf{C}^e - \mathbf{C}^d_{act}. \tag{61}$$

The stress/elastic-strain relationship then takes the form

$$\boldsymbol{\sigma} = \mathbf{C}^{act} : \boldsymbol{\varepsilon}^e. \tag{62}$$

If all three principal strains ε_i are tensile, then we have $\mathbf{C}^{act} = \mathbf{C}$. On the other hand, if all ε_i are compressive, then $\mathbf{C}^{act} = \mathbf{C}^e$; i.e. the local microcrack is entirely closed under current state. It is noted that Ortiz (1985) proposed similar treatment to accommodate the active "added compliance" tensor. The results of the two treatments, however, are not equivalent since the inversion procedure destroys the equivalency. □

Remark 4.2.5. The anisotropic damage model presented in this section is based on tensile brittle failure mode. For some brittle materials such as concrete, however, both tensile and compressive failure modes can occur. To accommodate this phenomenon, eqn (56) can be modified, following an approach in Ortiz (1985) (see eqn (3.18) therein), as follows to account for both tensile and compressive strain contributions:

$$\dot{\mathbf{C}} = -\dot{\xi}^{+} H^{+} \mathbf{P}^{+} \mathbf{C}^{0} \mathbf{P}^{+} - \dot{\xi}^{-} H^{-} \mathbf{P}^{-} \mathbf{C}^{0} \mathbf{P}^{-} \tag{63}$$

where the superscripts "+" and "−" signify the tensile and compressive damage evolution quantities, respectively. In addition, $\mathbf{P} \equiv \mathbf{I} - \mathbf{P}^{+}$. Therefore, tensile and compressive microcrack initiation and growth can develop simultaneously and separately (at different rates). □

Remark 4.2.6. Due to anisotropic damage evolution, an originally isotropic material becomes fully anisotropic, and the associated Poisson's ratio becomes a second-order anisotropic tensor. □

5. COMPUTATIONAL ALGORITHMS FOR DAMAGE MODELS

Numerical integration algorithms for the proposed elastoplastic-damage evolution equations are systematically explored in this section within the context of the finite element method. Use of the "operator split method" leads to a class of simple and efficient constitutive algorithms. In particular, new three-step operator split algorithms are presented for the proposed damage models. Strain softening and localization issues concerning damage models are also addressed.

5.1. *Inviscid isotropic damage algorithm*

We first summarize the locally averaged elastoplastic-damage rate constitutive equations.

$$\dot{\boldsymbol{\varepsilon}} = \nabla^{s}\dot{\mathbf{u}}(t)$$

$$\begin{cases} \dot{d}_{t} = \dot{\mu} H \\ \dot{r}_{t} = \dot{\mu} \\ \dot{\mu} \geqslant 0, \quad g(\xi_{t}, r_{t}) \leqslant 0, \quad \dot{\mu} g(\xi_{t}, r_{t}) = 0 \end{cases}$$

$$\dot{\boldsymbol{\sigma}} = \frac{\mathrm{d}}{\mathrm{d}t}\left[(1-d)\frac{\partial \Psi^{e}(\boldsymbol{\varepsilon}^{e}, \mathbf{q})}{\partial \boldsymbol{\varepsilon}^{e}}\right] \tag{64}$$

$$\begin{cases} \dot{\boldsymbol{\varepsilon}}^{p} = \dot{\lambda}\dfrac{\partial f}{\partial \bar{\boldsymbol{\sigma}}}(\bar{\boldsymbol{\sigma}}, \mathbf{q}) \\ \dot{\mathbf{q}} = \dot{\lambda}\mathbf{h}(\bar{\boldsymbol{\sigma}}, \mathbf{q}) \\ \dot{\lambda} \geqslant 0, \quad f(\bar{\boldsymbol{\sigma}}, \mathbf{q}) \leqslant 0, \quad \dot{\lambda} f(\bar{\boldsymbol{\sigma}}, \mathbf{q}) = 0 \end{cases}$$

where ξ is the damage energy release rate.

From an algorithmic point of view, the problem of integrating the evolution equations (64) amounts to updating the basic variables $\{\boldsymbol{\sigma}, d, \boldsymbol{\varepsilon}^{p}, \mathbf{q}\}$ in a fashion consistent with the constitutive model. It is important to realize that during this updating process the history of strains $t \to \boldsymbol{\varepsilon} \equiv \nabla^{s}\mathbf{u}(t)$ is assumed to be given.

Equations of evolution (64) are to be solved incrementally over a sequence of given time steps $[t_{n}, t_{n+1}] \subset \mathbb{R}_{+}$, $n = 0, 1, 2, \ldots$. Thus, the initial conditions for eqn (64) are

$$\{\boldsymbol{\sigma}, d, \boldsymbol{\varepsilon}^{p}, \mathbf{q}\}|_{t=t_{n}} = \{\boldsymbol{\sigma}_{n}, d_{n}, \boldsymbol{\varepsilon}_{n}^{p}, \mathbf{q}_{n}\}. \tag{65}$$

In accordance with the notion of operator split, we consider an additive decomposition of eqn (64) into the following elastic, plastic, and damage parts.

Elastic part	*Plastic part*	*Damage part*
$\dot{\boldsymbol{\varepsilon}} = \nabla^S \dot{\mathbf{u}}(t)$	$\dot{\boldsymbol{\varepsilon}} = \mathbf{0}$	$\dot{\boldsymbol{\varepsilon}} = \mathbf{0}$
$\dot{d} = 0$	$\dot{d} = 0$	$\dot{d} = \begin{cases} \dot{\xi} H & \text{iff } g_t = \dot{g}_t = 0 \\ 0 & \text{otherwise} \end{cases}$
$\dot{r} = 0$	$\dot{r} = 0$	$\dot{r} = \begin{cases} \dot{\xi} & \text{iff } g_t = \dot{g}_t = 0 \\ 0 & \text{otherwise} \end{cases}$
$\dot{\boldsymbol{\sigma}} = (1-d)\dfrac{\partial^2 \Psi^e}{\partial \boldsymbol{\varepsilon}^{e2}} : \dot{\boldsymbol{\varepsilon}}$	$\dot{\boldsymbol{\sigma}} = -(1-d)\dfrac{\partial^2 \Psi^e}{\partial \boldsymbol{\varepsilon}^{e2}} : \dot{\boldsymbol{\varepsilon}}^p$	$\dot{\boldsymbol{\sigma}} = -\dot{d}\dfrac{\partial \Psi^e}{\partial \boldsymbol{\varepsilon}^e}$
$\dot{\boldsymbol{\varepsilon}}^p = \mathbf{0}$	$\dot{\boldsymbol{\varepsilon}}^p = \dot{\lambda}\dfrac{\partial f}{\partial \bar{\boldsymbol{\sigma}}}(\bar{\boldsymbol{\sigma}}, \mathbf{q})$	$\dot{\boldsymbol{\varepsilon}}^p = \mathbf{0}$
$\dot{\mathbf{q}} = \mathbf{0}$	$\dot{\mathbf{q}} = \dot{\lambda}\mathbf{h}(\bar{\boldsymbol{\sigma}}, \mathbf{q})$	$\dot{\mathbf{q}} = \mathbf{0}.$ (66a–c)

It is noted that the three columns of (66) do indeed add up to eqn (64), in agreement with the notion of operator split (see Chorin *et al.*, 1978). Further, the first two columns of eqn (66) define the classical elastoplastic problem (with damage variable d fixed) and the corresponding computational algorithm reduces to the elastic predictor/plastic corrector scheme. In what follows we give a step-by-step efficient integration procedure.

5.1.1. *Elastic predictor.* An algorithm consistent with problem (66a), referred to as the "elastic predictor" in the sequel, is given by the following process.

(i) Strain update. Given the incremental displacement field $\mathbf{u}_{n+1}$, the strain tensor is updated at Gauss points as

$$\boldsymbol{\varepsilon}_{n+1} = \boldsymbol{\varepsilon}_n + \nabla^S \mathbf{u}_{n+1}. \tag{67}$$

(ii) Elastic trial stress. By merely performing function evaluation (no iteration), we obtain

$$\boldsymbol{\varepsilon}^{p\,\text{trial}}_{n+1} = \boldsymbol{\varepsilon}^p_n; \quad \mathbf{q}^{\text{trial}}_{n+1} = \mathbf{q}_n; \quad d^{\text{trial}}_{n+1} = d_n \tag{68}$$

$$\boldsymbol{\sigma}^{\text{trial}}_{n+1} = (1-d_n)\frac{\partial \Psi^e(\boldsymbol{\varepsilon}_{n+1} - \boldsymbol{\varepsilon}^p_n, \mathbf{q})}{\partial \boldsymbol{\varepsilon}^e}; \quad \bar{\boldsymbol{\sigma}}^{\text{trial}}_{n+1} = \frac{\boldsymbol{\sigma}^{\text{trial}}_{n+1}}{(1-d_n)}. \tag{69}$$

5.1.2. *Plastic corrector.* To develop an algorithm consistent with the plastic part (66b), the plastic yield condition is checked first.

(iii) Check for yielding

$$f(\bar{\boldsymbol{\sigma}}^{\text{trial}}_{n+1}, \mathbf{q}^{\text{trial}}_{n+1}) \begin{cases} \leqslant 0 \ \textbf{elastic} \Rightarrow \text{go to step (v)} \\ > 0 \ \textbf{plastic} \Rightarrow \text{return mapping.} \end{cases} \tag{70}$$

(iv) Plastic return mapping corrector. In the case of plastic loading, predictor stresses and internal variables are "returned back" to the yield surface along the algorithmic counterpart of the flow generated (66b). One typically employs either the closest-point-projection or cutting plane algorithms (see, e.g. Simo and Ju, 1987a, b). Once the plastic consistency condition (in effective stress space) is enforced, state variables at the end of plastic corrector phase become

$$\{\bar{\boldsymbol{\sigma}}_{n+1}, d_n, \boldsymbol{\varepsilon}^p_{n+1}, \mathbf{q}_{n+1}\}. \tag{71}$$

It should be noted that all existing return mapping algorithms for elastoplasticity become directly applicable (with no modification) in our elastoplastic-damage formulation.

5.1.3. *Damage corrector.* To complete the product formula algorithm, it remains to develop an algorithm consistent with the damage part (66c) which operates on initial conditions (71) to produce the final state $\{\sigma_{n+1}, d_{n+1}, \varepsilon^p_{n+1}, \mathbf{q}_{n+1}\}$.

(v) Damage evolution. Compute "damage energy release rate" ξ_{n+1} according to

$$\xi_{n+1} \equiv \Psi^{(1)}(\varepsilon^e_{n+1}, \mathbf{q}_{n+1}) \tag{72}$$

where $\varepsilon^e_{n+1} \equiv \varepsilon_{n+1} - \varepsilon^p_{n+1}$. The damage variable d_{n+1} and damage threshold r_{n+1} are then given by

$$d_{n+1} = \begin{cases} d_n & \text{if } \xi_{n+1} - r_n \leqslant 0 \\ d_n + (\xi_{n+1} - \xi_n) H_{n+1} & \text{otherwise} \end{cases} \tag{73}$$

$$r_{n+1} \equiv \max\{r_n, \xi_{n+1}\} \tag{74}$$

$$\sigma_{n+1} = (1 - d_{n+1})\bar{\sigma}_{n+1}. \tag{75}$$

It is emphasized that no iteration is required in the damage correction phase. Although plasticity and damage are coupled in rate equations (64), the algorithmic treatment renders uncoupled plasticity and damage algorithms. The simplicity and efficiency of the overall procedure are noteworthy.

5.2. *Rate-dependent isotropic damage algorithm*

The rate-dependent damage mechanism described in Section 3.4 can be efficiently implemented to obtain consistent and accurate incremental solutions. In this section, a one-parameter family of unconditionally stable integration algorithm is presented. Let us assume that damage loading is taking place; i.e. $g \equiv \xi_{n+1} - r_n > 0$. By applying the generalized mid-point rule to eqn (35) we have

$$\begin{aligned} &\varepsilon^e_{n+\alpha} \equiv \alpha\varepsilon^e_{n+1} + (1-\alpha)\varepsilon^e_n; \quad \xi_{n+\alpha} \equiv \Psi^{(1)}(\varepsilon^e_{n+\alpha}, \mathbf{q}_{n+\alpha}) \\ &r_{n+\alpha} \equiv \alpha r_{n+1} + (1-\alpha) r_n; \quad d_{n+\alpha} = d_n + \Delta\mu_{n+\alpha} g_{n+\alpha} H_{n+\alpha} \\ &r_{n+\alpha} = r_n + \Delta\mu_{n+\alpha} g_{n+\alpha} \equiv r_n + \Delta\mu_{n+\alpha}(\xi_{n+\alpha} - r_{n+\alpha}) \end{aligned} \tag{76}$$

where $\alpha \in [0, 1]$ and $\Delta\mu_{n+\alpha} \equiv \mu(t_{n+\alpha} - t_n)$. The amount of expansion experienced by the damage surface during the time step is computed from (76) by solving for r_{n+1}:

$$r_{n+\alpha} = \frac{[1 - (1-\alpha)\Delta\mu_{n+\alpha}] r_n + \Delta\mu_{n+\alpha}\xi_{n+1}}{1 + \alpha\Delta\mu_{n+\alpha}}, \quad (\alpha \geqslant \tfrac{1}{2}). \tag{77}$$

From elementary numerical analysis, we note that algorithm (76), (77) is unconditionally stable for $\alpha \geqslant \frac{1}{2}$ and second-order accurate for $\alpha = \frac{1}{2}$. Typically, the value $\alpha = 1$ corresponding to a backward-Euler finite difference scheme is employed. We will restrict our attention to this case in the ensuing development. The elastic predictor and plastic corrector are identical to the previous derivation shown in Section 5.1. Only the damage corrector phase needs modification to account for rate dependency. The numerical integration scheme for rate-dependent damage corrector is summarized for convenience in Table 1 for the fully implicit case ($\alpha = 1$).

It is interesting to examine two limiting values $\mu \to 0$ and $\mu \to \infty$ of the damage viscosity coefficient, and their effect on the evolution of r_{n+1} and g_{n+1}.

(a) For $\mu \to 0$ (so that $\Delta\mu_{n+1} \to 0$), we obtain $r_{n+1} \to r_n$ and $g_{n+1} \to (\xi_{n+1} - r_n)$. Hence, no further damage takes place during the time increment and (in the absence of plastic flow) one has instantaneous elastic response.

(b) For $\mu \to \infty$ (so that $\Delta\mu_{n+1} \to \infty$), we have $r_{n+1} \to \xi_{n+1}$, $g_{n+1} \to 0$, and $\Delta d_{n+1} = \Delta\xi_{n+1} H_{n+1}$. This situation corresponds to the rate-independent damage character-

Table 1. Rate-dependent damage corrector algorithm

(1) Compute current "damage energy release rate" ξ_{n+1} according to

$$\xi_{n+1} \equiv \Psi^e(\boldsymbol{\varepsilon}^e_{n+1}, \mathbf{q}_{n+1}).$$

(2) Check the damage loading criterion: $g(\xi_{n+1}, r_n) \equiv \xi_{n+1} - r_n > 0$?
YES: rate-dependent damage loading. Proceed to (3).
NO: no further damage within this time step. Exit.

(3) Compute r_{n+1} and $\Delta\mu_{n+1} g_{n+1}$:

$$\Delta\mu_{n+1} = \mu \Delta t_{n+1}$$

$$r_{n+1} = \frac{[r_n + \Delta\mu_{n+1}\xi_{n+1}]}{[1 + \Delta\mu_{n+1}]}$$

$$\Delta\mu_{n+1} g_{n+1} \equiv \Delta r_{n+1} = \frac{\Delta\mu_{n+1}}{1 + \Delta\mu_{n+1}} (\xi_{n+1} - r_n).$$

(4) Update damage parameter and stress:

$$\Delta d_{n+1} = \Delta\mu_{n+1} g_{n+1} H_{n+1}$$

$$d_{n+1} = d_n + \Delta d_{n+1}$$

$$\boldsymbol{\sigma}_{n+1} = (1 - d_{n+1}) \bar{\boldsymbol{\sigma}}_{n+1}.$$

ization. Hence, as $\mu \to \infty$ we recover the inviscid damage model characterized in Section 3.2. Note that since $0 \leqslant \mu \leqslant \infty$ we must have $r_n \leqslant r_{n+1} \leqslant \xi_{n+1}$; namely, the expansion of the damage surface is properly bounded between the instantaneous elasticity and the inviscid damage limit.

5.3. *Anisotropic damage algorithm*

The operator splitting methodology developed in Section 5.1 can be immediately extended to accommodate anisotropic brittle damage mechanism outlined in Section 4.2. The three-step operator split is as follows.

Elastic part	*Plastic part*	*Damage part*
$\dot{\boldsymbol{\varepsilon}} = \nabla^S \dot{\mathbf{u}}(t)$	$\dot{\boldsymbol{\varepsilon}} = \mathbf{0}$	$\dot{\boldsymbol{\varepsilon}} = \mathbf{0}$
$\dot{\mathbf{C}} = \mathbf{0}$	$\dot{\mathbf{C}} = \mathbf{0}$	$\dot{\mathbf{C}} = \begin{cases} -\xi H \mathbf{P}^+ \mathbf{C}^o \mathbf{P}^+ & \text{iff } g_t = \dot{g}_t = 0 \\ 0 & \text{otherwise} \end{cases}$
$\dot{r} = 0$	$\dot{r} = 0$	$\dot{r} = \begin{cases} \xi & \text{iff } g_t = \dot{g}_t = 0 \\ 0 & \text{otherwise} \end{cases}$
$\dot{\boldsymbol{\sigma}} = \mathbf{C} : \dot{\boldsymbol{\varepsilon}}$	$\dot{\boldsymbol{\sigma}} = -\mathbf{C} : \dot{\boldsymbol{\varepsilon}}^p$	$\dot{\boldsymbol{\sigma}} = \dot{\mathbf{C}} : \boldsymbol{\varepsilon}^e$
$\dot{\boldsymbol{\varepsilon}}^p = \mathbf{0}$	$\dot{\boldsymbol{\varepsilon}}^p = \dot{\lambda} \dfrac{\partial f}{\partial \bar{\boldsymbol{\sigma}}} (\bar{\boldsymbol{\sigma}}, \mathbf{q})$	$\dot{\boldsymbol{\varepsilon}}^p = \mathbf{0}$
$\dot{\mathbf{q}} = \mathbf{0}$	$\dot{\mathbf{q}} = \dot{\lambda} \mathbf{h}(\bar{\boldsymbol{\sigma}}, \mathbf{q})$	$\dot{\mathbf{q}} = \mathbf{0}.$

(78a–c)

Computationally, the only modification needed concerns the anisotropic damage corrector, now involving an eigen-calculation to compute the positive (tensile) projection of the strain tensor.

5.3.1. *Anisotropic damage corrector.* Step (v) outlined in Section 5.1 is modified as follows.

(v) Damage evolution
(a) Perform the spectral decomposition:

$$\boldsymbol{\varepsilon}_{n+1} = \sum_{i=1}^{3} \varepsilon_i \mathbf{p}_i \otimes \mathbf{p}_i. \tag{79}$$

(b) Compute $\mathbf{Q}_{n+1}$ and $\mathbf{Q}^{+}_{n+1}$:

$$\mathbf{Q}_{n+1} = \sum_{i=1}^{3} \mathbf{p}_i \otimes \mathbf{p}_i; \quad \mathbf{Q}^{+}_{n+1} = \sum_{i=1}^{3} \hat{H}(\varepsilon_i)\mathbf{p}_i \otimes \mathbf{p}_i. \tag{80}$$

Recall that $\hat{H}(\cdot)$ denotes the Heaviside step function.

(c) Compute the projection tensor $\mathbf{P}^{+}_{n+1}$ and the elastic tensile strain tensor $\boldsymbol{\varepsilon}^{e+}_{n+1}$:

$$\mathbb{P}^{+}_{ijkl} = Q^{+}_{ia} Q^{+}_{jb} Q_{ka} Q_{lb}; \quad \boldsymbol{\varepsilon}^{e+}_{n+1} = \mathbf{P}^{+}_{n+1} : \boldsymbol{\varepsilon}^{e}_{n+1}. \tag{81}$$

(d) Compute the damage energy release rate ξ_{n+1} according to eqn (54).

(e) Update anisotropic secant (unloading) stiffness modulus according to eqns (55), (56):

$$\mathbf{C}_{n+1} = \begin{cases} \mathbf{C}_n & \text{if } \tilde{G}(\xi_{n+1}, s, a, c, \rho) - r_n \leqslant 0 \\ \mathbf{C}_n - (\xi_{n+1} - \xi_n) H_{n+1} \mathbf{P}^{+}_{n+1} \mathbf{C}^0 \mathbf{P}^{+}_{n+1} & \text{otherwise} \end{cases} \tag{82}$$

(f) Update the damage threshold r_{n+1} and Cauchy stress $\boldsymbol{\sigma}_{n+1}$:

$$r_{n+1} \equiv \max \{r_n, \tilde{G}_{n+1}\} \tag{83}$$

$$\boldsymbol{\sigma}_{n+1} = \mathbf{C}_{n+1} : \boldsymbol{\varepsilon}^{e}_{n+1}. \tag{84}$$

Remark 5.3.1.1. A rate-dependent anisotropic damage algorithm can be constructed parallel to the rate-dependent isotropic damage algorithm in Table 1. □

5.4. *Strain softening and localization*

It is now well known that there are uniqueness, well-posedness and numerical convergence problems associated with apparent "strain-softening" computations due to the loss of material strong ellipticity. As a result, finite element computations exhibit spurious mesh sensitivity when the mesh size goes to infinitesimal. These numerical difficulties may be overcome by means of the nonlocal damage theory (see, e.g. Eringen and Edelen, 1972; Baxant *et al.*, 1987; Xia *et al.*, 1987), or viscous damage model presented in Section 3.4. The nonlocal damage characterization is physically very appealing at the microscale. However, experimental determination of the characteristic length l and the weighting function ω may be major problems. Recently, nevertheless, Bazant and Pijaudier-Cabot (1988) proposed an interesting method to determine the characteristic length from experimental data. Further, nonlocal computation is to some extent incompatible with local finite element calculation and further enhancement in consistency and accuracy is needed. On the other hand, the proposed viscous damage mechanism is not only suitable for accommodating dynamic rate effect but also offers a possibility for controlling loss of ellipticity.

In particular, following a line of argument due to Valanis (1985), it can be shown that a viscous damage model of the type (35) satisfies the positiveness condition in Valanis (1985) and therefore leads to well-posed initial-value problems. To this end, we take differentiation of the relation $\boldsymbol{\sigma} = (1-d)\bar{\boldsymbol{\sigma}}$ and use eqn (35) to obtain

$$\begin{aligned} \dot{\boldsymbol{\sigma}} &= (1-d)\dot{\bar{\boldsymbol{\sigma}}} - \dot{d}\bar{\boldsymbol{\sigma}} \\ &= (1-d)\bar{\mathbf{C}}^{ep} : \dot{\boldsymbol{\varepsilon}} - \mu\langle g \rangle H \bar{\boldsymbol{\sigma}}. \end{aligned} \tag{85}$$

We recall that $\bar{\boldsymbol{\sigma}} = \partial \Psi^{a}(\boldsymbol{\varepsilon}^{e}, \mathbf{q})/\partial \boldsymbol{\varepsilon}^{e}$ and $\bar{\mathbf{C}}^{ep}$ is the effective elastoplastic tangent stiffness given in eqn (27). At a state defined by $\{\boldsymbol{\varepsilon}, d, r\}$, for two different stress rates $\dot{\boldsymbol{\sigma}}_1$, $\dot{\boldsymbol{\sigma}}_2$, and two different strain rates $\dot{\boldsymbol{\varepsilon}}_1$ and $\dot{\boldsymbol{\varepsilon}}_2$, it follows from (85) that

$$(\dot{\boldsymbol{\sigma}}_1 - \dot{\boldsymbol{\sigma}}_2) : (\dot{\boldsymbol{\varepsilon}}_1 - \dot{\boldsymbol{\varepsilon}}_2) = (1-d)(\dot{\boldsymbol{\varepsilon}}_1 - \dot{\boldsymbol{\varepsilon}}_2) : \bar{\mathbf{C}}^{ep} : (\dot{\boldsymbol{\varepsilon}}_1 - \dot{\boldsymbol{\varepsilon}}_2) > 0 \tag{86}$$

provided that the undamaged elastoplastic tangent modulus $\bar{\mathbf{C}}^{ep}$ is positive definite and $d < 1$. Thus, the material is positive in the sense of Valanis (1985).

In recent years, the applicability and limitations of distributed damage models to brittle materials such as concrete have been questioned by some researchers (see, e.g. Read and Hegemier, 1984). The fundamental question is to what extent the softening that is observed experimentally (for a boundary-value-type sufficiently large specimen) is a manifestation of local material behavior or, on the contrary, a global structural (boundary-value) effect brought about by fracture (macrocracks) and strain localization (such as shear band formation). To answer this question, we really should separate the issue into two parts. The first part concerns the boundary-value-type experimental testing of specimens. The second part focuses on the local constitutive behavior (not boundary-value problem) within the framework of the unit cell-based "meso-mechanics", the concept of characteristic length, together with the self-consistent method or homogenization technique. It is noted that, in the case of concrete, the characteristic length is approximately three times the aggregate size according to Bazant and Pijaudier-Cabot (1988), and a unit cell contains approximately 30–100 aggregates according to Krajcinovic and Fanella (1986).

For a sufficiently large (bigger than the unit cell) experimental specimen, the observed force–displacement curve indeed represents the global boundary-value-type response, rather than the local stress–strain behavior of a material element. In fact, in this boundary-value problem, there are three factors contributing to the apparent softening which is observed experimentally. These factors include: (a) the nucleation and growth of many distributed microcracks in the specimen, leading to local material softening in the sense of unit cell based meso-mechanics; (b) the strain localization phenomenon, resulting from the loss of ellipticity and stability of materials (see, e.g. Ortiz, 1987b); (c) the formation and propagation of global boundary-value-type macrocracks which are the direct products of microcrack coalescence in the specimen. Based on the above statements, this writer agrees with those researchers who concluded that true material softening is *less* than the apparent global softening observed in experiments. Therefore, strictly speaking, the global force displacement curve should not be directly interpreted as the local stress strain curve of a material element.

On the other hand, within a statistically representative unit cell (meso-mechanics), distributed microcracks and strain softening (at the meso-scale) do make sense since distributed microcracks (within the unit cell) do induce stiffness degradation and strain softening. One can factually apply the self-consistent method or the homogenization technique to compute the degradation of elastic and plastic material properties of a unit cell. These computations are, of course, related to the scale of the characteristic length of a material. Further, the so-called "size effects" (see, e.g. Sabnis and Mirza, 1979; Bazant, 1984; Fanella and Krajcinovic, 1988) are also closely related to the scale of characteristic length.

In summary, distributed damage models are suitable for modeling distributed (many) microcracks and material responses (not necessarily softening) in structural members before macrocracks become globally dominant. After the microcracks coalesce to form macrocracks, one can switch to fracture mechanics approaches provided that one takes into account: (i) the damage process zones in front of macrocracks (i.e. the macrocrack–microcrack interactions), and (ii) the damage-induced stiffness degradation and anisotropy in many (distributed) unit cells. Without these accounts, the resulting fracture calculations are not realistic nor meaningful. Conversely, direct application of a distributed damage model to solve a problem involving a single dominant macrocrack (in a boundary-value setting) is not likely to yield accurate results regarding macrocrack geometry and macrocrack opening displacement. Finally, distributed damage models are not directly suitable for predicting localization instability in materials.

6. APPLICATION TO CONCRETE AND MORTAR. EXPERIMENTAL VALIDATION

Concrete is a three-phase cementitious composite material composed of aggregate, mortar and interface zone (see, e.g. Mehta, 1986). Each of the three phases is itself multiphase in nature. For example, each aggregate particle may contain several minerals, and mortar is actually a mixture of cement paste and sand particles. Further, concrete has microcracks in the interface zone even before a structure is first loaded due to bleeding,

shrinkage, cement hydration heat, etc. The interface zone between the aggregate particle and mortar is typically 10–50 μm thick around large aggregates and is in general weaker than either aggregate or mortar. Due to this strength-limiting phase, the strength of concrete is considerably lower than that of mortar or aggregate.

Under compressive loading, microcracks initiate and propagate in the interface zone at low stress level, signifying a low energy barrier Ψ'' in the interface. These microcracks become unstable and propagate until they are arrested by cement paste matrix which has a higher value of debonding (damage) energy barrier Ψ'. When the stress level is above 50% of the ultimate strength, matrix (mortar) microcracks initiate and gradually spread until they join the microcracks originating from the interface zone. The coalesced crack system then becomes continuous. The crack system may be arrested by aggregate, but may also lead to rupture of local materials. Most stable microcracks are of the size of aggregate facets. Hence, aggregate size is closely related to the characteristic length of concrete. Considerable damage energy is needed for the formation and extension of matrix microcracks under a compressive load. By contrast, under tensile loading much less damage energy is required to initiate and propagate microcracks in matrix and interface zone. Therefore, concrete fails in brittle fashion in tension mode and is much tougher (more ductile) in compression failure mode. It is also recognized that plasticity (permanent deformation) in concrete is primarily due to the extended microcrack surfaces which are not completely closed even under unloading.

Without resorting to multi-phase mixture theories and models, we employ either isotropic or anisotropic damage models in the following sections to simulate microcrack initiation and growth in the interface zone and mortar matrix of concrete. Experimental validation involves both rate-independent and rate-dependent concrete testing data. In addition, microstructural factors such as the average aggregate size/spacing ratio are considered in the microcrack kinetic equations.

6.1. *Experimental validation of isotropic damage model*

The isotropic energy-based damage mechanism developed in Section 3 is specialized in this section to capture basic features of the behavior of concrete and mortar within bounds of experimental error. A two-invariant cap plasticity model originally proposed by DiMaggio and Sandler (1971) (see also Sandler *et al.*, 1976; Sandler and Rubin, 1979; Simo *et al.*, 1988) is employed to account for the plastic behavior of concrete. In view of the present shortcomings of experimental techniques and the wide scattering in available experimental data for concrete and mortar, a precise quantitative evaluation of the predicting capabilities of a given constitutive model does not seem to be warranted. Instead, it is felt that an overall qualitative reproduction of the main features of material behavior should play a dominant role in material modeling.

In particular, the kinetic law of microcrack growth, eqn (16) reduces to the following form:

$$\dot{d} = (k+\tfrac{1}{2})\dot{\xi}\tilde{H}(\xi, c, \rho) \tag{87}$$

where $k \equiv a/s$ is the average aggregate size/spacing ratio. Note that if aggregates are infinitely far away from one another, then k is 0. On the other hand, if aggregates are in contact, then k is 1. The bigger k is, the higher the aggregate/cement interface area density is and hence the faster the microcrack density grows. Certainly, eqn (87) is not a micromechanical kinetic equation. For exponentially growing progressive damage, the evolution function $\tilde{H}$ is assumed to be

$$\tilde{H}(\xi, c, \rho) \equiv \frac{\xi_0(1-A)}{\xi^2} + AB \exp\,[B(\xi_0 - \xi)]. \tag{88}$$

Here A and B are characteristic material parameters (implicit functions of c and ρ), and ξ_0 denotes the characteristic initial damage threshold. These parameters can be estimated in

a systematic manner from suitable experimental data. The average aggregate size/spacing factor k is taken as 0.7 for the following concrete specimens.

6.1.1. *Colorado concrete data.* The data for the following examples are taken from the well-documented experimental program conducted at the University of Colorado (see Scavuzzo *et al.*, 1983) on a systematic three-dimensional testing of concrete ($f'_c \approx 4$ ksi). The program consists of six major series of non-conventional multiaxial cyclic stress–strain curves. It is noted that replicate tests were run for some experiments, which enable us to assess the relative consistency of experimental data. The numerical results reported below not only include fitting of the model to complicated 3-D stress paths but, in addition, predictions of material behavior obtained by exercising the model against experimental results.

Circular stress path tests. Tests 3-3 and 3-4 are replicates concerning the following loading paths. The specimens are first subjected to hydrostatic monotonic loading to a specified deviatoric plane, followed by deviatoric loading along the triaxial compression path until completion of the specific circular path. The model parameters are obtained by optimal fitting with respect to test 3-3. These model parameters are then employed in the subsequent simulation intended to predict the behavior observed in the replicate test 3-4 under significant experimental data perturbations. In spite of considerable data corruption, good overall predictive capability of the model is observed, as illustrated in Figs 3 and 4. To demonstrate the effect of the aggregate size/spacing factor k on damage growth, three hypothetical k values ($k = 0.1, 0.5, 0.9$) are further employed to simulate test 3-3; see Fig. 5. It is clear that as k increases, microcrack density increases and therefore stress response degrades.

Cyclic simple shear tests. Tests 2-3 and 2-4 are intended to explore concrete response to deviatoric simple shear cycles with stress reversal about the hydrostatic state. Material parameter estimation is performed with respect to test 2-4, and prediction is exercised for test 2-3 (replicate). The results are shown in Figs 6 and 7. The overall qualitative agreement between simulations and experiments is satisfactory.

6.1.2. *Uniaxial compression tests.* In this example, we perform two replicate uniaxial unconfined compression tests of mortar (with $f'_c \approx 12$ ksi). The composition of mortar is as follows: cement 649 g, water 195 g, sand 150 g, plasticizer 9.1 ml. Ottawa sand with a fineness modulus of 2.11 is employed. The gradation is as follows: 33.33% retained on sieve gauge 30, 77.77% retained on sieve gauge 50 and 100% retained on sieve gauge 100.

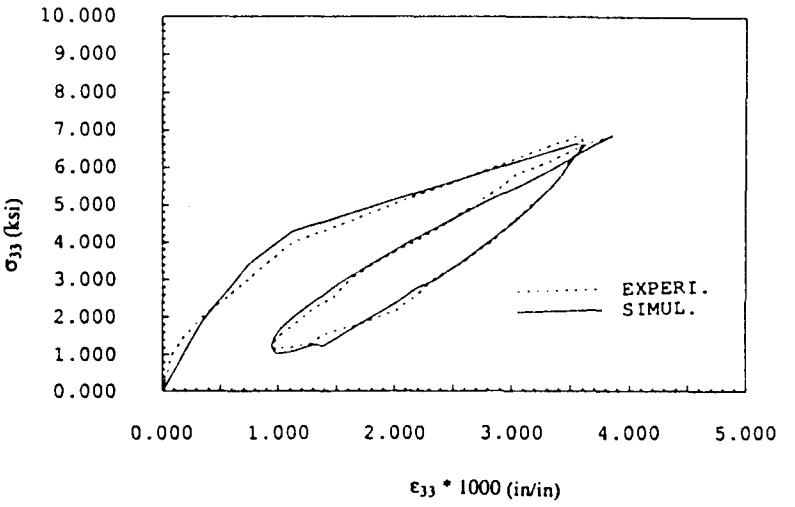

Fig. 3. Comparison of the experimental and isotropic simulated (fitted) data for Colorado concrete test 3-3.

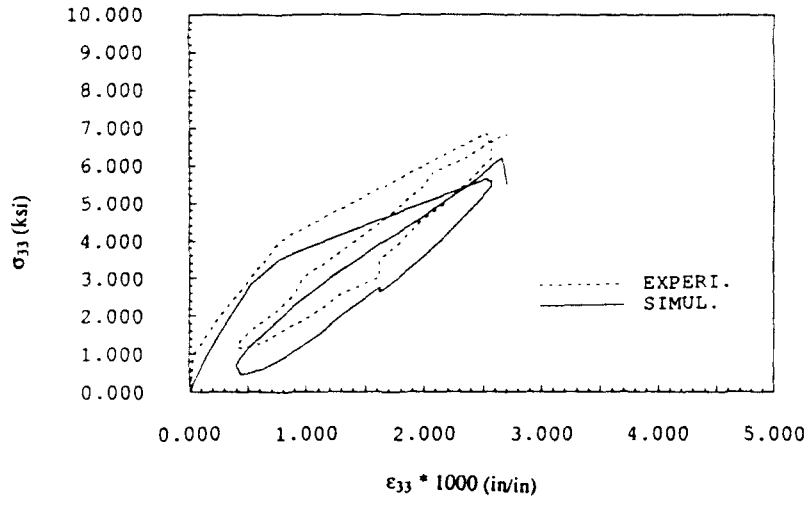

Fig. 4. Comparison of the experimental and isotropic simulated (predicted) data for Colorado concrete test 3-4.

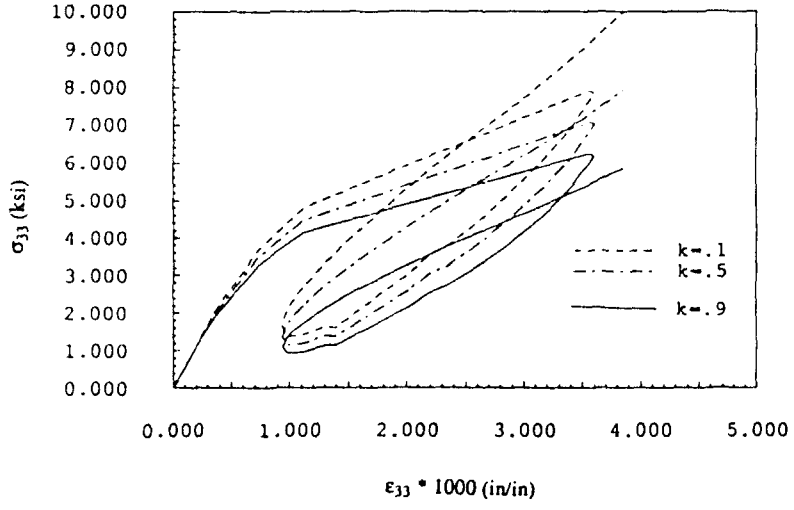

Fig. 5. Demonstration of the effect of the aggregate size/spacing factor k on the damage growth and stress response for test 3-3.

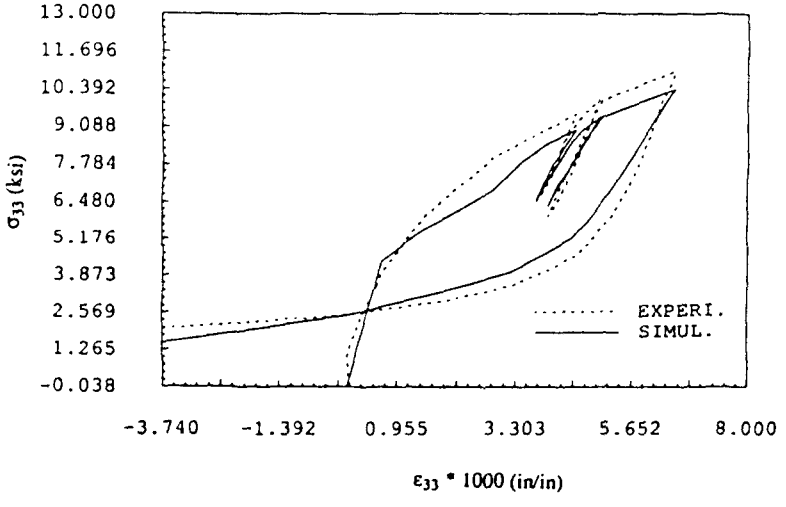

Fig. 6. Comparison of the experimental and isotropic simulated (fitted) data for Colorado concrete test 2-4.

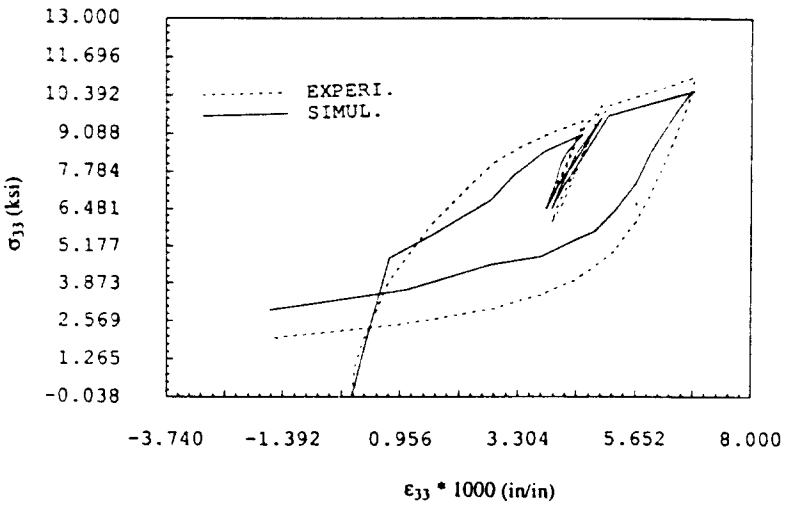

Fig. 7. Comparison of the experimental and isotropic simulated (predicted) data for Colorado concrete test 2-3.

Material parameters are obtained by optimal fitting with respect to test "M1" and prediction is carried out for test "M2"; see Figs 8 and 9. The effect of the inclusion size/spacing factor k (sand concentration) on damage growth can be seen again from Fig. 10 in which three hypothetical k values ($k = 0.1, 0.5, 0.9$) are employed to simulate test "M1".

6.2. *Experimental validation of rate-dependent isotropic damage model*

Two dynamic uniaxial compression concrete tests (Suaris and Shah, 1983, 1984) are considered in this section based on the rate-dependent isotropic damage algorithm given in Table 1. Two different constant strain rates are employed: fast loading ($\dot{\varepsilon} = 0.088$ sec $^{-1}$) and slow loading ($\dot{\varepsilon} = 1.0e-6$ sec $^{-1}$). The static uniaxial compressive strength is estimated to be 6.8 ksi.

Figure 11 shows experimental and simulated results at two strain rates. Good qualitative and quantitative agreement between the model and the experimental data is obtained. The rate enhancement of stress response due to the viscous damage mechanism is clearly demonstrated. That is, growth of microcracks is retarded at higher strain rates.

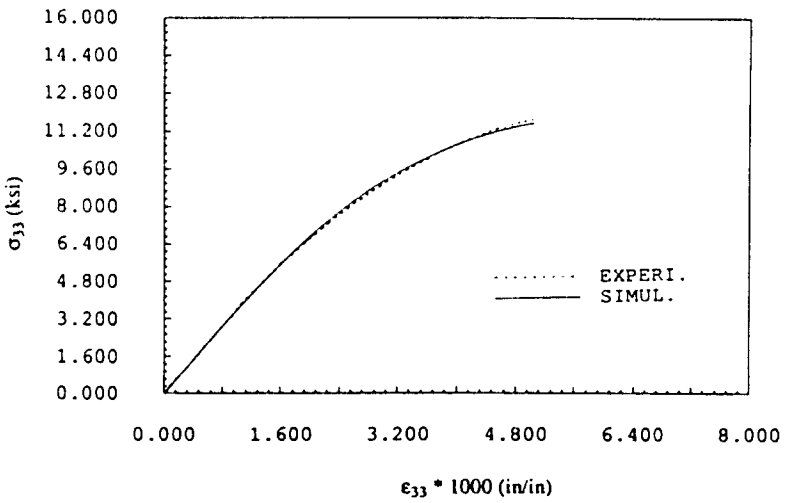

Fig. 8. Comparison of the experimental and isotropic simulated (fitted) data for uniaxial compression mortar test "M1".

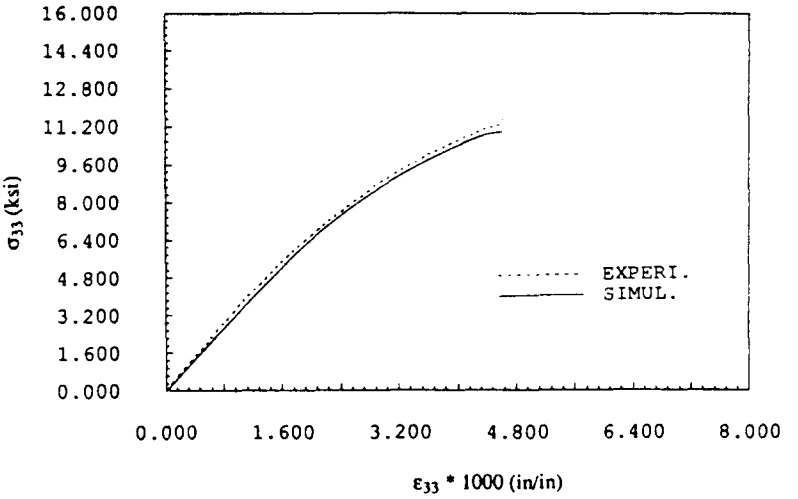

Fig. 9. Comparison of the experimental and isotropic simulated (predicted) data for uniaxial compression mortar test "M2".

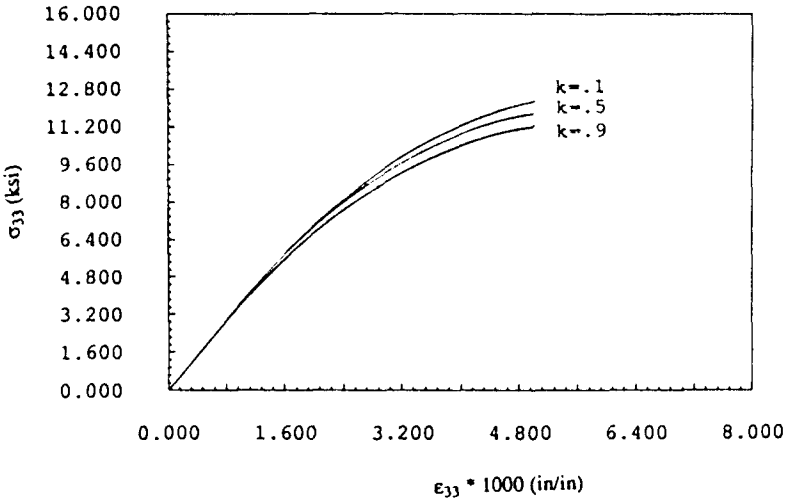

Fig. 10. Demonstration of the effect of the aggregate size spacing factor k on the damage growth and stress response for test "M1".

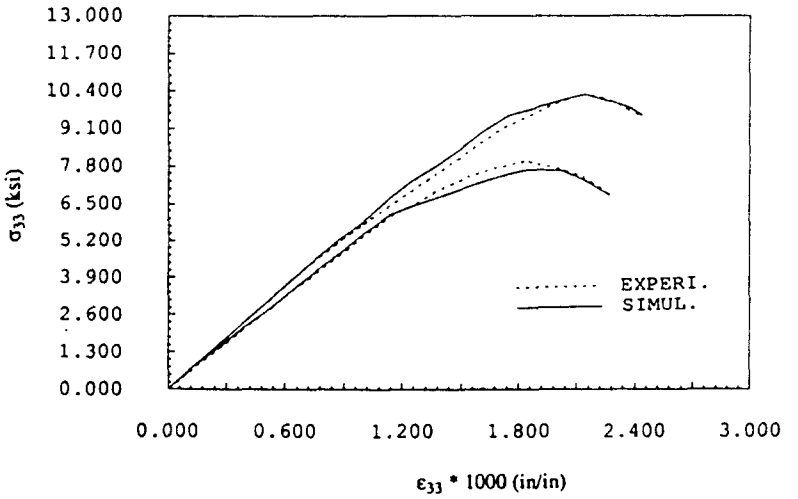

Fig. 11. Comparison of the experimental and isotropic simulated dynamic stress-strain curves for uniaxial compression test of concrete specimens.

6.3. *Experimental validation of anisotropic damage model*

The fourth-order anisotropic damage mechanism presented in Section 4.2 is employed next to simulate anisotropic damage growth in mortar. We recall from eqn (63) in Remark 4.2.5 that tensile and compressive strains can independently contribute to microcrack evolution. The uniaxial unconfined compression mortar tests previously considered in Section 6.1 are taken as examples again in this section. Under uniaxial compression, the fourth-order anisotropic damage mechanism reduces to an orthotropic damage mechanism and the reproduction of the "splitting mode" of cylindrical specimens is sought.

Since the tensile strength f_t' is approximately one-tenth of the compressive strength f_c', it appears reasonable to assume that the compressive microcrack growth rate (in the axial direction) is approximately 10% of the tensile (mode I) microcrack growth rate (in the lateral direction). As a consequence of the orthogonal eigenprojections ($\mathbf{P}^+$ and $\mathbf{P}^-$) and different growth rates, microcracks develop in the lateral and axial directions progressively and independently. In particular, microcracks form rapidly along axes parallel to the axis of loading, reduce the lateral stiffness gradually, and ultimately lead to the splitting failure mode. Experimental and numerical results for tests "M1" and "M2" are shown in Figs 12 and 13. In addition, the apparent Poisson's ratios for tests "M1" and "M2" are displayed in Figs 14 and 15. It is emphasized that microcrack growth and stiffness degradation in the

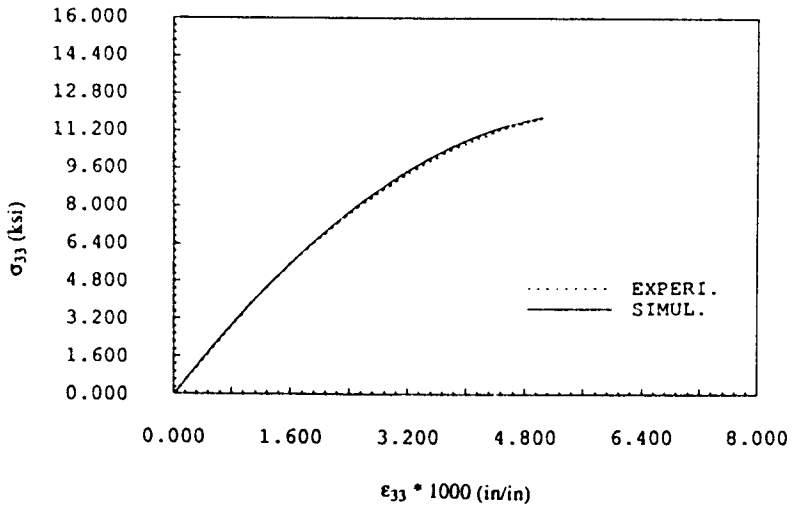

Fig. 12. Comparison of the experimental and anisotropic simulated (fitted) data for uniaxial compression mortar test "M1".

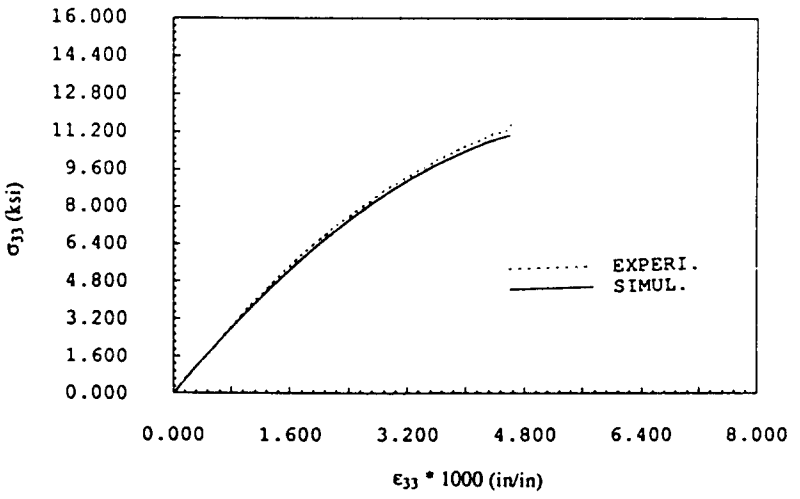

Fig. 13. Comparison of the experimental and anisotropic simulated (predicted) data for uniaxial compression mortar test "M2".

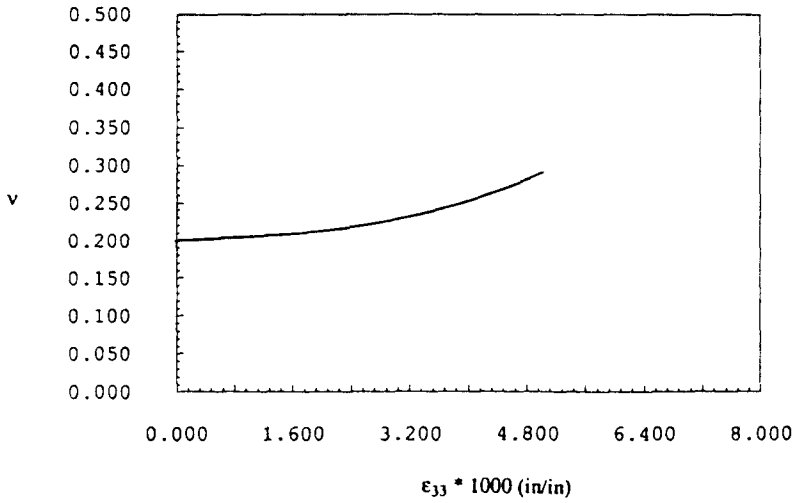

Fig. 14. Apparent Poisson's ratio for the mortar test "M1".

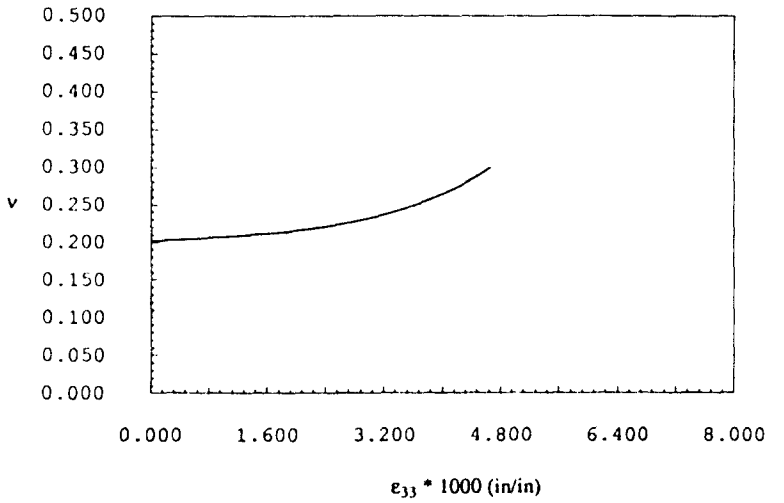

Fig. 15. Apparent Poisson's ratio for the mortar test "M2".

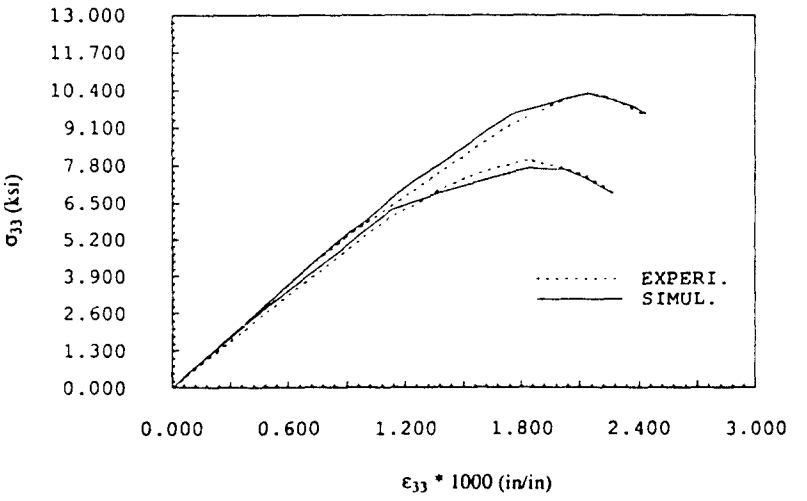

Fig. 16. Comparison of the experimental and anisotropic simulated dynamic stress–strain curves for uniaxial compression test of concrete specimens.

lateral direction is much much faster than that in the axial direction due to our anisotropic damage mechanism.

6.4. *Experimental validation of rate-dependent anisotropic damage model*

We re-examine the rate-dependent concrete tests previously discussed in Section 6.2 by a rate-dependent anisotropic damage model (see Remark 5.3.1.1). Again, microcracks develop rapidly along axes parallel to the axis of loading, and the splitting failure mode is obtained. Experimental and numerical results for two different rates ($\dot{\varepsilon} = 0.088$ sec^{-1} and $\dot{\varepsilon} = 1.0e-6$ sec^{-1}) are shown in Fig. 16. The capability of the proposed mechanism to simulate rate dependency and "splitting modes" of cylindrical concrete specimens is noteworthy.

7. CLOSURE

A number of energy-based isotropic and anisotropic damage models have been proposed in this paper to characterize microcrack initiation and growth in ductile and brittle materials. Thermodynamic basis, general nonlinear response, strain rate dependency, damage threshold, damage kinetic law, microcrack opening and closing, coupling of damage and plasticity, and anisotropic (brittle) damage mechanism have been presented within the general framework of damage mechanics, unit cell and homogenization concept. Damage initiation and propagation are linked to the (locally averaged) "total undamaged strain energy" $\Psi^0(\varepsilon^e, \mathbf{q})$, which is checked against the debonding energy (current damage threshold) required for unstable microcrack growth. It is noted that in the current literature damage models are either simply elastic-damageable or containing improper elastoplastic-damage thermodynamics and mechanisms.

Another essential purpose of the present work is to demonstrate that the proposed classes of elastoplastic-damage constitutive equations are well suited for large scale computation in spite of their sophistication. Use of the operator splitting methodology leads to three-step integration algorithms which, in addition to isotropic and anisotropic damage, are capable of accommodating general elastic–plastic response.

Experimental validation of the proposed models against concrete and mortar specimens is also given. We observe good qualitative and quantitative agreement between experimental data for concrete and mortar and the proposed models. In particular, softening behavior is well captured. Micromechanically based damage theories will be objectives of our future research.

Acknowledgements—This work was sponsored by the Air Force Office of Scientific Research under Grant No. AFOSR-88-0324, together with the Defense Nuclear Agency. This support and the interest and comments of Dr Spencer Wu and Dr Kent Goering are gratefully acknowledged.

REFERENCES

Ashby, M. F. (1979). Micromechanism of fracture in static and cyclic failure. In *Fracture Mechanics: Current Status, Future Prospects*. Proceedings of conference, Cambridge University, March 1979, pp. 1–27.

Bakhtar, K. *et al.* (1985). Concrete material properties. TerraTek Research, *DNA Concrete Meeting*, April 1985, Utah.

Bazant, Z. P. [1984]. Size effect in blunt fracture: concrete, rock, and metal. *J. Engng Mech. ASCE* **110**, 518–535.

Bazant, Z. P., Lin, F. B. and Pijaudier-Cabot, G. (1987). Yield limit degradation: nonlocal continuum model with local strain. In *Proc. Int. Conf. on Composite Plastics*, pp. 1757–1780, 6–10 April 1987, Barcelona, Spain.

Bazant, Z. P. and Pijaudier-Cabot, G. (1988). Nonlocal continuum damage and measurement of characteristic length. In *Mechanics of Composite Materials*—1988, pp. 79–86. Proc. Joint ASME/SES Conf., 20–22 June1988, Berkeley, CA.

Budiansky, B. and O'Connel, R. J. (1976). Elastic moduli of a cracked solid. *Int. J. Solids Structures* **12**, 81–97.

Chaboche, J. L. (1974). Une loi différentielle d'endommagement de fatigue avec cumulation non linéaire. *Rev. Fr. Méc.* **50, 51**.

Chaboche, J. L. (1981). Continuous damage mechanics—a tool to describe phenomena before crack initiation. *Nucl. Engng Des* **64**, 233–247.

Chaboche, J. L. (1982). Le concept de contrainte effective appliqué à l'élasticité et à la viscoplasticité en présence d'un endommagement anisotrope. *Mechanical Behavior of Anisotropic Solids*. Proc. EUROMECH Colloque 115, June 1979 (Edited by J. P. Boehler), pp. 737–760. Martinus Nijhoff.

Chorin, A., Hughes, T. J. R., McCracken, M. F. and Marsden, J. E. (1978). Product formulas and numerical algorithms. *Commun. Pure Appl. Math.* **31**, 205–256.

Chow, C. L. and Wang, J. (1987a). An anisotropic theory of continuum damage mechanics for ductile fracture. *Engng Fract. Mech.* **27**, 547–558.

Chow, C. L. and Wang, J. (1987b). An anisotropic continuum damage theory and its application to ductile crack initiation. In *Proc. ASME Winter Annual Meeting* (Edited by A. S. D. Wang and G. K. Haritos), pp. 1–9. 13–18 December 1987, Boston, MA.

Coleman, B. D. and Gurtin M. (1967). Thermodynamics with internal variables. *J. Chem. Phys.* **47**, 597–613.

Cordebois, J. P. and Sidoroff, F. (1979). Damage induced elastic anisotropy. *Mechanical Behavior of Anisotropic Solids*. Proc. EUROMECH Colloque 115, June 1979 (Edited by J. P. Boehler), pp. 761–774. Martinus Nijhoff.

Cordebois, J. P. and Sidoroff, F. (1982). Endommagement anisotrope en élasticité et plasticité. *J. Méc. Théor. Appl.* No. spécial, pp. 45–59.

DiMaggio, F. L. and Sandler, I. S. (1971). Material models for granular solids. *J. Engng Mech. Div. ASCE* **97**, 935–950.

Dragon, A. (1985). Plasticity and ductile fracture damage: study of void growth in metals. *Engng Fract. Mech.* **21**, 875–885.

Dragon, A. and Chihab, A. (1985). On finite damage: ductile fracture-damage evolution. *Mech. Mater.* **4**, 95–106.

Eringen, A. C. (1968). Mechanics of micromorphic continua. In *Mechanics of Generalized Continua* (Edited by E. Kroner), pp. 18–35. Springer.

Eringen, A. C. (1983). Interaction of a dislocation with a crack. *J. Appl. Phys.* **54**, 6811–6817.

Eringen, A. C. (1987). Theory of nonlocal elasticity and some applications. *Res. Mechanica* **21**, 313–342.

Eringen, A. C. and Edelen, D. G. B. (1972). On nonlocal elasticity. *Int. J. Engng Sci.* **10**, 233–248.

Fanella, D. and Krajcinovic, D. (1988). Size effect in concrete. *J. Engng Mech. ASCE* **114**, 704–715.

Francois, D. (1984). Fracture and damage mechanics of concrete. *Application of Fracture Mechanics to Cementitious Composites*. NATO Advanced Research Workshop, 4–7 September 1984, Northwestern University (Edited by S. P. Shah), pp. 97–110.

Grady, D. E. and Kipp, M. E. (1980). Continuum modelling of explosive fracture in oil shale. *Int. J. Rock Mech. Min. Sci. Geomech. Abstr.* **17**, 147–157.

Hill, R. (1967). The essential structure of constitutive laws for metal composites and polycrystals. *J. Mech. Phys. Solids* **15**, 79–95.

Hill, R. (1972). On constitutive macro-variables for heterogeneous solids at finite strain. *Proc. R. Soc. Lond., Ser. A* **326**, 131–147.

Horii, H. and Nemat-Nasser, S. (1983). Overall moduli of solids with microcracks: load induced anisotropy. *J. Mech. Phys. Solids* **31**, 155–171.

Hult, J. (1974). Creep in continua and structures. In *Topics in Applied Continuum Mechanics*. Springer, Vienna.

Ilankamban, R. and Krajcinovic, D. (1987). A constitutive theory for progressively deteriorating brittle solids. *Int. J. Solids Structures* **23**, 1521–1534.

Ju, J. W., Monteiro, P. J. M. and Rashed, A. I. (1989). On continuum damage of cement paste and mortar as affected by porosity and sand concentration. *J. Engng Mech. ASCE* **115**, 105–130.

Ju, J. W., Simo, J. C., Pister, K. S. and Taylor, R. L. (1987). A parameter estimation algorithm for inelastic material models. In *Proc. Second Int. Conf. and Short Course on Constitutive Laws for Engineering Materials: Theory and Applications* (Edited by C. S. Desai *et al.*), pp. 1233–1240, 5–10 January 1987, Tucson, AZ.

Kachanov, L. M. (1958). Time of the rupture process under creep conditions. *IVZ Akad Nauk*, S.S.R., Otd Tech Nauk, No. 8, pp. 26–31.

Kachanov, M. (1980). Continuum model of medium with cracks. *J. Engng Mech. Div. ASCE* **106**, 1039–1051.

Kachanov, M. (1981). Crack growth under conditions of creep and damage. In *Creep in Structures* (Edited by A. Ponter and D. Hayhurst), pp. 520–524. Springer, Berlin.

Kachanov, M. (1982). A microcrack model of rock inelasticity. Part I. *Mech. Mater.* **1**, 19–27, 1039–1051.

Kachanov, M. (1984). On brittle fracture of a thin plastic interlayer in creep conditions. In *Mechanics of Material Behavior* (Edited by G. Dvorak and R. Shield), pp. 191–200. Elsevier, Amsterdam.

Kachanov, M. (1987a). Elastic solids with many cracks: a simple method of analysis. *Int. J. Solids Structures* **23**, 23–43.

Kachanov, M. (1987b). On modelling of anisotropic damage in elastic brittle materials – a brief review. In *Proc. ASME Winter Annual Meeting* (Edited by A. S. D. Wang and G. K. Haritos), pp. 99–105. 13–18 December 1987, Boston, MA.

Krajcinovic, D. (1983a). Creep of structures – a continuous damage mechanics approach. *ASME J. Struct. Mech.* **11**, 1–11.

Krajcinovic, D. (1983b). Constitutive equations for damaging materials. *ASME J. Appl. Mech.* **50**, 355–360.

Krajcinovic, D. (1985). Constitutive theories for solids with defective microstructure. In *Damage Mechanics and Continuum Modeling* (Edited by N. Stubbs and D. Krajcinovic), pp. 39–56. ASCE.

Krajcinovic, D. (1987). Micromechanical basis of phenomenological models. In *Continuum Damage Mechanics: Theory and Application* (Edited by D. Krajcinovic and J. Lemaitre). Springer (to appear).

Krajcinovic, D. and Fanella, D. (1986). A micromechanical damage model for concrete. *Engng Fract. Mech.* **25**, 585–596.

Krajcinovic, D. and Fonseka, G. U. (1981) The continuous damage theory of brittle materials, Parts I and II. *ASME J. Appl. Mech.* **48**, 809–824.

Leckie, F. and Hayhurst, D. (1974). Creep rupture of structures. *Proc. R. Soc. Lond. Ser. A* **240**, 323.

Lemaitre, J. (1971). Evaluation of dissipation and damage in metals. *Proc. I.C.M.* (1), Kyoto, Japan.

Lemaitre, J. (1984). How to use damage mechanics. *Nucl. Engng Des.* **80**, 233–245.

Lemaitre, J. (1985). A continuous damage mechanics model for ductile fracture. *J. Engng Mater. Technol.* **107**, 83–89.

Lemaitre, J. (1986). Plasticity and damage under random loading. In *Proc. Tenth U.S. National Congress of Applied Mechanics* (Edited by J. P. Lamb), pp. 125–134. 16–20 June 1986. Austin, TX. ASME.

Lemaitre, J. and Chaboche, J. L. (1974). A nonlinear model of creep-fatigue damage cumulation and interaction. *Proc. IUTAM Symp. of Mechanics of Visco-elastic Media and Bodies*. Springer, Gothenburg.
Lemaitre, J. and Chaboche, J. L. (1978). Aspects phénoménologiques de la rupture par endommagement. *J. Méc. Appl.* **2**, 317–365.
Lemaitre, J. and Dufailly, J. (1977). Modélisation et identification de l'endommagement plastique des métaux. 3ème Congrès Francais de Mécanique, Grenoble.
Lemaitre, J. and Plumtree, A. (1979). Application of damage concepts to predict creep-fatigue failures. *J. Engng Mater. Technol.* **101**, 284–292.
Loland, K. E. (1980). Continuous damage model for load-response estimation of concrete. *Cement Concrete Res.* **10**, 395–402.
Lorrain, M. and Loland, K. E. (1983). Damage theory applied to concrete. *Fracture Mechanics of Concrete* (Edited by F. H. Wittmann), pp. 341–369. Elsevier.
Marigo, J. J. (1985). Modeling of brittle and fatigue damage for elastic material by growth of microvoids. *Engng Fract. Mech.* **21**, 861–874.
Mazars, J. (1982). Mechanical damage and fracture of concrete structures. In *Advances in Fracture Research* (*Fracture* 81), Vol. 4, pp. 1499–1506. Pergamon Press.
Mazars, J. (1986). Description of the behavior of composite concretes under complex loadings through continuum damage mechanics. In *Proc. Tenth U.S. National Congress of Applied Mechanics* (Edited by J. P. Lamb), pp. 135–139. 16–20 June 1986. Austin, TX. ASME.
Mazars, J. and Lemaitre, J. (1984). Application of continuous damage mechanics to strain and fracture behavior of concrete. *Application of Fracture Mechanics to Cementitious Composites*, NATO Advanced Research Workshop, 4–7 September 1984. Northwestern University (Edited by S. P. Shah), pp. 375–388.
Mehta, P. K. (1986). Concrete: Structure, Properties, and Materials. Prentice-Hall Inc., Englewood Cliffs, N.J.
Murakami, S. (1981). Effects of cavity distribution in constitutive equations of creep and creep damage. EUROMECH Colloque on Damage Mechanics, Cachan, France.
Ortiz, M. (1985). A constitutive theory for the inelastic behavior of concrete. *Mech. Mater.* **4**, 67–93.
Ortiz, M. (1987a). A method of homogenization of elastic media. *Int. J. Engng Sci.* **25**, 923–934.
Ortiz, M. (1987b). An analytical study of the localized failure modes of concrete. *Mech. Mater.* **6**, 159–174.
Ortiz, M. and Simo, J. C. (1986). An analysis of a new class of integration algorithms for elastoplastic constitutive relations. *Int. J. Numer. Meth. Engng* **23**, 353–366.
Perzyna, P. (1966). Fundamental problems in viscoplasticity. *Adv. Appl. Mech.* **9**, 244–368.
Pijaudier-Cabot, G. and Bazant, Z. P. (1987). Nonlocal damage theory. *J. Engng Mech. ASCE* **113**, 1512–1533.
Rabotnov, I. N. (1963). On the equations of state for creep. *Progress in Applied Mechanics—the Prager Anniversary Volume*, pp. 307–315.
Read, H. E. and Hegemier, G. A. (1984). Strain softening of rock, soil and concrete—a review article. *Mech. Mater.* **3**, 271–294.
Resende, L. and Martin, J. B. (1984). A progressive damage continuum model for granular materials. *Composite Meth. Appl. Mech. Engng* **42**, 1–18.
Sabnis, G. M. and Mirza, S. M. (1979). Size effects in model concretes. *J. Struct. Div. ASCE* **105**, 1007–1020.
Sandler, I. S., DiMaggio, F. L. and Baladi, G. Y. (1976). Generalized cap model for geological materials. *J. Geotech. Engng Div. ASCE* **102**, 683–699.
Sandler, I. S. and Rubin D. (1979). An algorithm and a modular subroutine for the cap model. *Int. J. Numer. Analyt. Meth. Geomech.* **3**, 173–186.
Scavuzzo, R., Stankowski, T., Gerstle, K. H. and Ko, H. Y. (1983). Stress-strain curves for concrete under multiaxial load histories. NSF CME-80-01508, Department of Civil Engineering, University of Colorado, Boulder.
Simo, J. C. and Ju, J. W. (1987a). Stress and strain based continuum damage models—I. Formulation. *Int. J. Solids Structures* **23**, 821–840.
Simo, J. C. and Ju, J. W. (1987b). Stress and strain based continuum damage models—II. Computational aspects. *Int. J. Solids Structures* **23**, 841–869.
Simo, J. C. and Ju, J. W. (1976c). On continuum damage-elastoplasticity at finite strains: a computational framework. *Comput. Mech.* (in press).
Simo, J. C., Ju, J. W., Pister, K. S. and Taylor, R. L. (1988). An assessment of the cap model: consistent return algorithms and rate-dependent extension. *J. Engng Mech. ASCE* **114**, 191–218.
Suaris, W. and Shah, S. P. (1983). Properties of concrete subjected to impact. *J. Struct. Engng ASCE* **109**, 1727–1741.
Suaris, W. and Shah, S. P. (1984). Rate-sensitive damage theory for brittle solids. *J. Engng Mech. ASCE* **110**, 985–997.
Sumarac, D. and Krajcinovic, D. (1987). A self-consistent model for microcrack-weakened solids. *Mech. Mater.* **6**, 39–52.
Takeda, J. and Tachikawa, H. (1971). Deformation and fracture of concrete subjected to dynamic load. In *Proc. Int. Conf. Mechanical Behavior of Materials*, Vol. 4, *Concrete and Cement Paste, Glass and Ceramics*, pp. 267–277. 15–20 August 1971, Kyoto, Japan.
Talreja, R. (1985). A continuum mechanics characterization of damage in composite materials. *Proc. R. Soc. Lond., Ser. A* **399**, 195–216.
Terrien, M. (1980). Emission acoustique et comportement mécanique post-critique d'un béton sollicité en traction. *Bulletin de Liaison des laboratoires des Ponts et Chaussées*, No. 105, pp. 65–72.
Vakulenko, A. A. and Kachanov, M. L. (1971). Continuum theory of medium with cracks. *Mekh. Tverdogo Tela* **4**, 159–166.
Valanis, K. C. (1985). On the uniqueness of solution of the initial value problem in softening materials. *J. Appl. Mech.* **52**, 649–653.
Weitsman, Y. (1987). Coupled damage and moisture-transport in fiber-reinforced, polymeric composites. *Int. J. Solids Structures* **23**, 1003–1025.
Wu, C. H. (1985). Tension compression test of a concrete specimen via a structure damage theory. In *Damage Mechanics and Continuum Modelling* (Edited by N. Stubbs and D. Krajcinovic), pp. 1–12. ASCE.
Xia, S., Li, G. and Lee, H. (1987). A nonlocal damage theory. *Int. J. Fract.* **34**, 239–250.